






Article

Novel Benzothiazole-Based Ureas as 17 β -HSD10 Inhibitors, A Potential Alzheimer's Disease Treatment

Laura Aitken ^{1,*}, Ondrej Benek ^{2,3,*}, Brogan E. McKelvie ¹, Rebecca E. Hughes ⁴, Lukas Hroch ², Monika Schmidt ³, Louise L. Major ⁵, Lucie Vinklarova ³, Kamil Kuca ³, Terry K. Smith ⁵, Kamil Musilek ^{2,3} and Frank J. Gunn-Moore ¹

¹ University of St. Andrews, School of Biology, Medical and Biological Sciences Building, North Haugh, St. Andrews KY16 9TF, UK

² University Hospital, Biomedical Research Center, Sokolska 581, 500 05 Hradec Kralove, Czech Republic

³ University of Hradec Kralove, Faculty of Science, Department of Chemistry, Rokitanskeho 62, 500 03 Hradec Kralove, Czech Republic

⁴ Cancer Research UK Edinburgh Centre, MRC Institute of Genetics and Molecular Medicine, Western General Hospital, University of Edinburgh, Edinburgh EH4 2XU, UK

⁵ Biomedical Science Research Complex, University of St. Andrews, North Haugh, St. Andrews KY16 9ST, UK

* Correspondence: la49@st-andrews.ac.uk (L.A.); ondrej.benek@uhk.cz (O.B.)

† These authors contributed equally to this work.

Received: 3 July 2019; Accepted: 25 July 2019; Published: 29 July 2019



Abstract: It has long been established that mitochondrial dysfunction in Alzheimer's disease (AD) patients can trigger pathological changes in cell metabolism by altering metabolic enzymes such as the mitochondrial 17 β -hydroxysteroid dehydrogenase type 10 (17 β -HSD10), also known as amyloid-binding alcohol dehydrogenase (ABAD). We and others have shown that frentizole and riluzole derivatives can inhibit 17 β -HSD10 and that this inhibition is beneficial and holds therapeutic merit for the treatment of AD. Here we evaluate several novel series based on benzothiazolylurea scaffold evaluating key structural and activity relationships required for the inhibition of 17 β -HSD10. Results show that the most promising of these compounds have markedly increased potency on our previously published inhibitors, with the most promising exhibiting advantageous features like low cytotoxicity and target engagement in living cells.

Keywords: Alzheimer's disease (AD); amyloid-beta peptide (A β); mitochondria; 17 β -hydroxysteroid dehydrogenase type 10 (17 β -HSD10); amyloid binding alcohol dehydrogenase (ABAD); benzothiazole

1. Introduction

There is a strong, well-documented connection between Alzheimer's disease (AD) and mitochondrial dysfunction [1–3]. Mitochondrial changes in AD patients are an early event, preceding the onset of amyloid plaque formation, and include morphology abnormalities and changes in metabolism stemming from alterations in the complexes of the electron transport chain, the enzymes in the tricarboxylic acid cycle (TCA), and changes in components of the mitochondrial membrane involved in import/export flux. Mitochondria are key to the production of adenosine triphosphate (ATP) via the metabolism of glucose and fatty acids. Mitochondrial dysfunction in AD includes activity changes in many enzymes involved in these processes and contributes to the reduction in energy metabolism in AD [4]. Mitochondrial dysfunction is also exacerbated by the presence of amyloid beta peptide (A β) within mitochondria [5]. One mitochondrial enzyme affected in AD is 17 β -HSD10 (17 β -hydroxysteroid dehydrogenase type 10, also known as amyloid- β binding alcohol dehydrogenase (ABAD) or 3-Hydroxyacyl-CoA dehydrogenase). 17 β -HSD10's primary role is to

utilise several substrates to produce energy in the β -fatty acid oxidation pathway, the energy source when glucose levels are low, playing a prominent role in AD, where glucose metabolism is significantly decreased [6]. Importantly, we and others have shown that inhibition of this enzyme is beneficial in both in vitro and in vivo AD models in its own right and also protects against A β toxicity in both cellular and transgenic mouse models of AD [7–12]. A current working hypothesis is that by inhibiting the enzyme activity of 17 β -HSD10 (a contributor to the β -fatty acid oxidation pathway) this can help re-balance alterations in glucose metabolism observed in AD (Aitken unpublished data).

17 β -HSD10 was first identified as an A β binding protein in 1997 [13], a finding which has subsequently been confirmed using a number of techniques [5,13,14]. 17 β -HSD10 is known to interact with the two major plaque forming isoforms of A β , namely A β (1–40) and A β (1–42), leading to distortion of the enzyme structure and inhibition of its normal function as an energy provider for cells [15,16]. In vitro experiments have shown that the interaction between 17 β -HSD10 and A β is cytotoxic and 17 β -HSD10's function is altered with a build-up of reactive oxygen species (ROS) and toxins leading to mitochondrial dysfunction. Using site-directed mutagenesis and surface plasmon resonance protein interaction assays (SPR), Lustbader et al. identified the L_D loop of the 17 β -HSD10 protein as the binding site for A β and subsequently synthesised a 28-amino acid peptide encompassing this region, which was termed the 17 β -HSD10 decoy peptide [5]. Using SPR assays it has been shown that this 17 β -HSD10 decoy peptide can prevent the binding of 17 β -HSD10 to A β (1–40) and A β (1–42). Significantly, inhibition of the interaction between 17 β -HSD10 and A β by the 17 β -HSD10-decoy peptide was shown to translate into a cytoprotective effect in cell culture experiments. Cortical neurons exposed to A β (1–42) showed a significant increase in cell death, as measured by cytochrome-c release, whilst those pre-incubated with the 17 β -HSD10 decoy peptide did not. Critically, for the first time, this work demonstrated that inhibition of the 17 β -HSD10-A β interaction may target potential disease-relevant mechanisms.

Other than the disruption of the 17 β -HSD10/A β interaction, there is a second approach which may hold merit in treating AD: the direct modulation of 17 β -HSD10 enzyme activity. In vitro experiments with neuronal-like SHSY-5Y cells exposed to the 17 β -HSD10 inhibitor AG18051, showed a reduction in mitochondrial dysfunction and oxidative stress associated with the interaction between 17 β -HSD10 and A β and protected the cells from A β -mediated cytotoxicity [7,8]. This proved that inhibiting 17 β -HSD10 activity may also be a viable therapeutic approach for the treatment of AD.

In our previously published work [9] we discuss the rationale behind utilising analogues of the FDA-approved drugs frentizole and riluzole as inhibitors of 17 β -HSD10 for potential therapeutics in AD. Briefly, many benzothiazole analogues have been shown to possess various biological activities in the central nervous system, with riluzole itself highlighted as neuroprotective. Thus, we focused on generating potent 17 β -HSD10 inhibitors based on the benzothiazole scaffold, identifying several potent inhibitors (Figure 1) [9].

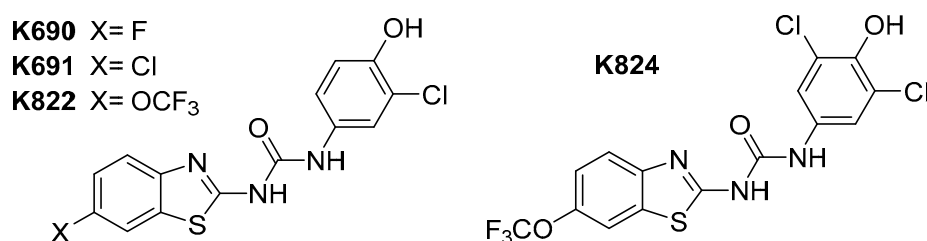


Figure 1. Structure of previously identified benzothiazolylurea inhibitors.

These compounds highlighted key structural features required for 17 β -HSD10 inhibition with the 6-trifluoromethoxy and 6-halogen substitution of the benzothiazole moiety and 3-chloro, 4-hydroxy substitution of the phenyl moiety proving the most favourable, however, with limited solubility the compounds were not optimal for cellular evaluation. The aim of this study was not only to generate benzothiazole urea scaffolds which would show improved potency, but to also generate compounds

with improved tolerance and less cytotoxicity within our cellular assays, i.e., better pharmacokinetic parameters. To that end, four series of compounds have been synthesised targeting the key areas of benzothiazole moiety, phenyl ring and urea linker (Figure 2).

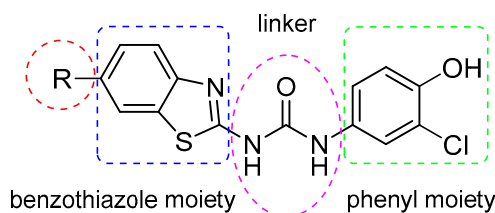


Figure 2. Design of benzothiazolylurea-based 17 β -HSD10 inhibitors.

2. Results and Discussion

2.1. Structural Design and Chemical Synthesis

The first series of compounds is a continuation of our previously reported work [9]. While the benzothiazole scaffold and urea linker were kept intact, further substitution changes into the distal phenyl ring were introduced, mainly at position 3 (Table 1). Methoxy substitutions at position 6 of benzothiazole were selected and based on the comparable inhibitory activity with halogenated analogues and due to the availability of starting material and improved physical chemical properties.

Table 1. First series of prepared compounds (2–11).

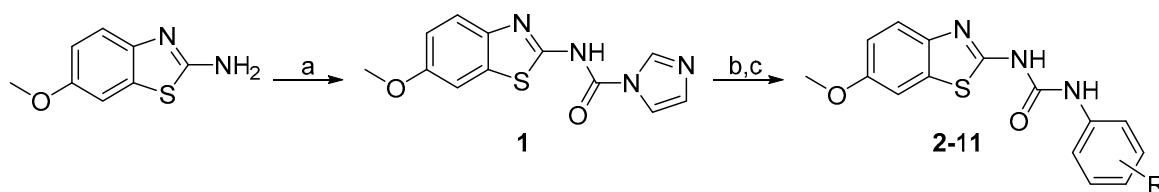
Compound ID	R ¹	R ²
2	Me	-OH
3	<i>t</i> -butyl	-OH
4	-CN	-OH
5	-Br	-OH
6	-I	-OH
7	-NH ₂	-OH
8	6-hydroxypyridin-3-yl ^a	-OH
9	-	-NH ₂
10	-Cl	-NH ₂
11	-Cl	-CH ₂ OH

^a Substitution pattern replacement of whole distal phenyl ring.

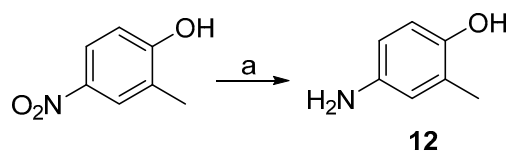
Benzothiazolylureas were formed using the two-step reaction process subsequently described. Initially, 6-methoxybenzo[*d*]thiazol-2-amine was activated with 1,1'-carbonyldiimidazole (CDI; Scheme 1a). Subsequently, intermediate **1** was reacted with corresponding substituted aniline (resp. 5-aminopyridin-2-ol for final product **8**) to give final di-substituted ureas (2–11). To obtain compounds **7**, **9** and **10**, *N*-Boc protective group was cleaved under acidic conditions (Scheme 1c) as the final step of their synthesis.

Most aniline derivatives were commercially available, but in several cases the aniline intermediates had to be prepared as further described:

In general, reduction of substituted nitrobenzenes into the corresponding anilines (e.g., **12**) was achieved with palladium on activated carbon (Pd/C) catalysed hydrogenation (Scheme 2).

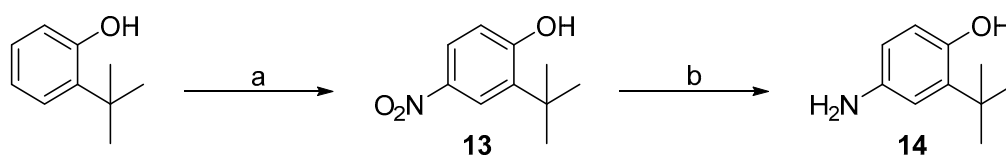


Scheme 1. Synthesis of 2–11. Reagents and conditions: (a) CDI, DCM, RT; (b) aniline derivative, MeCN, reflux; (c) 4 M HCl, dioxane, RT (for *N*-Boc protected intermediates).



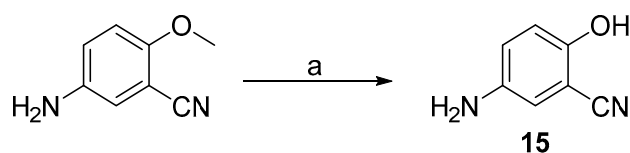
Scheme 2. Synthesis of aniline intermediate 12. Reagents and conditions: (a) Pd/C, H₂, EtOH, RT.

2-(*Tert*-butyl)phenol was selected as a starting material for introduction of *tert*-butyl group into the *meta* position of distal phenyl ring. Firstly, nitration was achieved with nitric acid in the presence of acetic acid as reaction solvent (Scheme 3a) to obtain intermediate 13. Secondly, the introduced nitro group was reduced to 4-amino-2-(*tert*-butyl)phenol (14). Initially, the reduction was attempted with Pd/C catalysed hydrogenation (Scheme 2). However, a complex mixture of decomposed starting material was received. Thus, reduction was accomplished using iron powder and ammonium chloride (Scheme 3b) to successfully obtain intermediate 14.



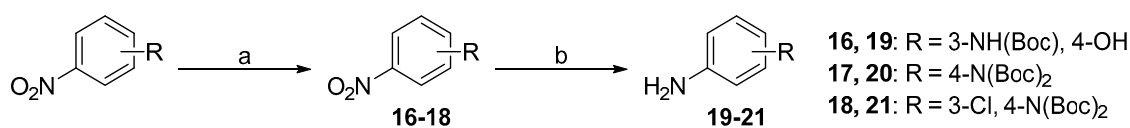
Scheme 3. Synthesis of intermediates 13 and 14. Reagents and conditions: (a) HNO₃/CH₃COOH, RT; (b) Fe, NH₄Cl, MeOH/H₂O, RT.

5-amino-2-hydroxybenzonitrile (15) was prepared from its methoxy analogue by demethylation using aluminium chloride (Scheme 4).



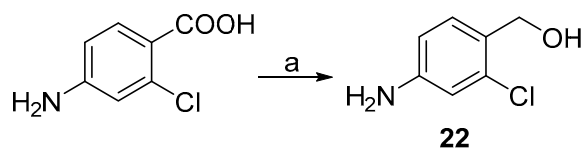
Scheme 4. Synthesis of intermediate 15. Reagents and conditions: (a) AlCl₃, DCM, reflux.

N-Boc (de)protection had to be performed in order to obtain final compounds with the free amine group on the distal phenyl ring. Firstly, the amine group of nitroaniline was protected with di-*tert*-butyl dicarbonate (Scheme 5a) to yield intermediates 16–18. Secondly, the nitro group was reduced with Pd/C catalysed hydrogenation to obtain intermediates 19–21 (Scheme 5b). Final *N*-Boc acidic deprotection was performed after the urea formation step (Scheme 1).



Scheme 5. Synthesis of intermediates 16–21. Reagents and conditions: (a) (Boc)₂O, DMAP, THF, RT; (b) Pd/C, H₂, EtOH, RT.

Aniline analogue with primary alcohol group in the *para* position (**22**) was generated via reduction of corresponding carboxylic acid with lithium aluminium hydride (Scheme 6).



Scheme 6. Synthesis of intermediate **22**. Reagents and conditions: (a) LiAlH₄, THF, −5 °C to RT.

The next series was focused on selected modifications in the linker region of the scaffold, while the original distal phenyl ring substitution (3-chlorine-4-hydroxy) was selected in combination with either 6-methoxy, 6-chlorine or unsubstituted benzothiazole ring (Table 2). Additionally, to compliment recently published work [8,17], dimethyl phosphonate analogues were prepared as standards (**34–36**) for comparison between inter-workgroup biological evaluations along with the most promising 3-chloro, 4-hydroxy substitution pattern. Finally, methylation of either one or both nitrogen atoms of the urea linker was conducted with the aim of constraining the conjugation between the two aromatic moieties.

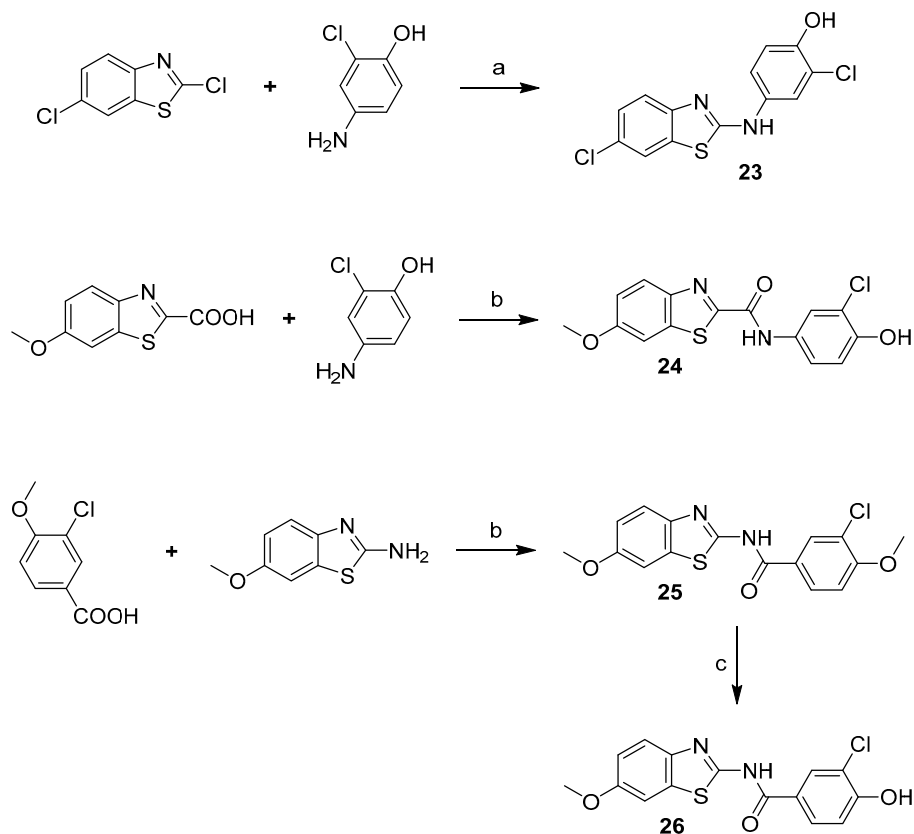
Table 2. Second series of prepared compounds (**23–49**).

Compound ID	R ¹	Linker	R ²
	Cl		3-Cl, 4-OH
24	OMe		3-Cl, 4-OH
26	OMe		3-Cl, 4-OH
28	OMe		3-Cl, 4-OH
29	OMe		3-OH, 4-OH
34	OMe		4-F
35	OMe		4-OH
36	OMe		3-COOCH ₃ , 4-OH
37	OMe		3-Cl, 4-OH

Table 2. Cont.

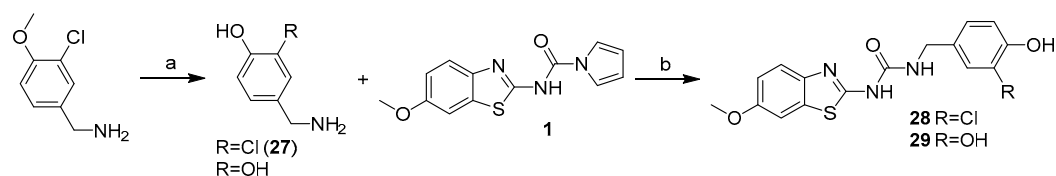
Compound ID	R ¹	Linker	R ²
41	-		3-Cl, 4-OH
45	-		3-Cl, 4-OH
46	OMe		3-Cl, 4-OH
49	-		3-Cl, 4-OH

Compound **23** with linker consisting of a secondary amine group was prepared by means of simple *N*-alkylation, and amides **24** and **25** were prepared in a reaction of corresponding carboxylic acid with CDI and corresponding amine. Compound **25** was subsequently *O*-demethylated to give the final product **26** (Scheme 7).



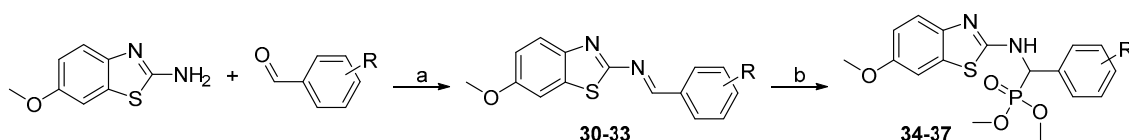
Scheme 7. Synthesis of compounds **23**–**26**. Reagents and conditions: (a) NMP, 160 °C; (b) CDI, DMF, RT; (c) AlCl₃, DCM, reflux.

Compounds **28** and **29** were prepared using the general procedure for urea linker synthesis in reaction with CDI (Scheme 8). In case of compound **28** synthesis, the corresponding benzylamine intermediate (**27**) was first prepared from its methoxy analogue by demethylation using AlCl_3 (Scheme 8).



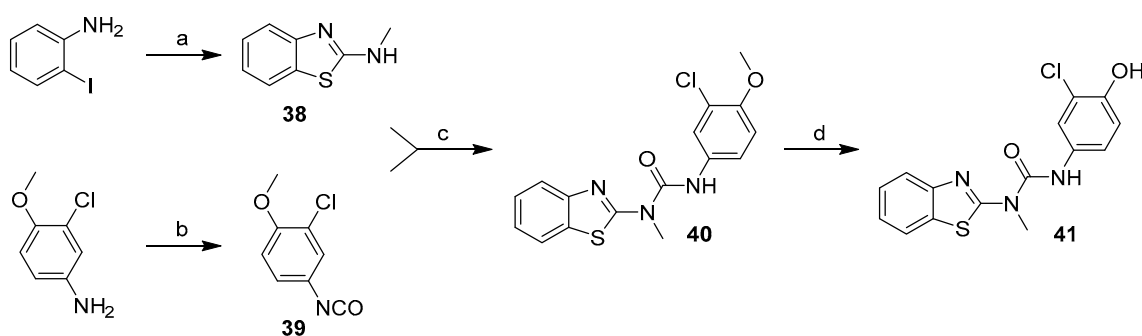
Scheme 8. Synthesis of compounds **27–29**. Reagents and conditions: (a) AlCl_3 , DCM, reflux; (b) MeCN, reflux.

While the originally used reaction conditions proved to be troublesome to produce the desired compounds [17], dimethyl phosphonates (**34–37**) were instead prepared in a two-step process. Firstly, 6-methoxybenzo[*d*]thiazol-2-amine and corresponding aldehyde were coupled at reflux conditions to obtain imines **30–33**, which were subsequently treated with dimethyl phosphite and 1,1,3,3-tetramethylguanidine to generate the final products in satisfactory yields (Scheme 9).



Scheme 9. Synthesis of phosphonate derivatives. Reagents and conditions: (a) toluene, reflux; (b) dimethyl phosphite, 1,1,3,3-tetramethylguanidine, THF, 65 °C.

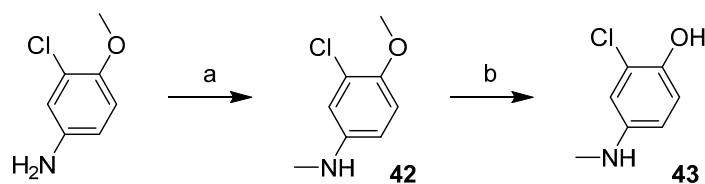
Compound **41** was prepared in four steps (Scheme 10). The benzothiazole moiety (**38**) was prepared from 2-iodoaniline in reaction with methylisothiocyanate and tetrabutylammonium bromide catalysed by copper (I) chloride [18]. 3-chloro-4-methoxyaniline was treated with triphosgene to give the isocyanate intermediate (**39**), which was then reacted with the benzothiazole moiety and the resulting methoxy derivative (**40**) was demethylated using AlCl_3 to give compound **41**.



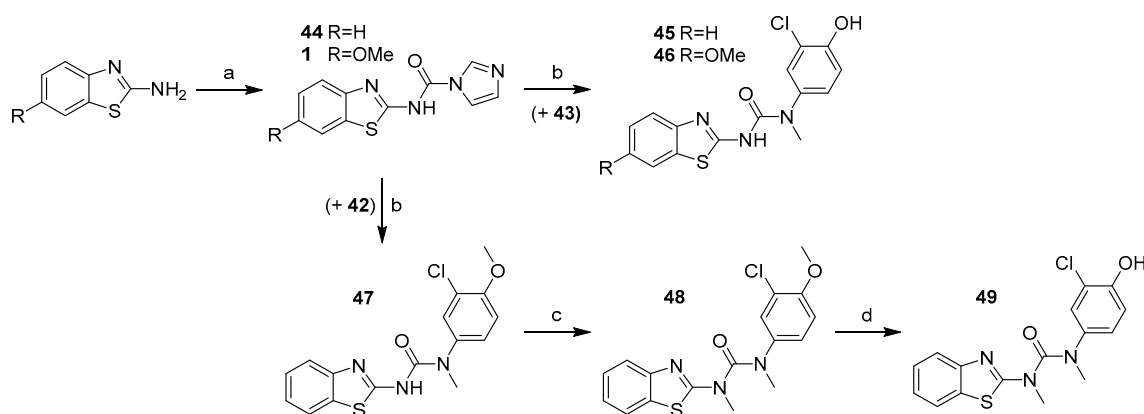
Scheme 10. Synthesis of compound **41**. Reagents and conditions: (a) MeNCS, TBABr, CuCl, DMSO, 60–80 °C; (b) triphosgene, Et_3N , DCM, 0 °C–reflux; (c) THF, RT; (d) AlCl_3 , toluene, reflux.

The first step in the synthesis of products **45**, **46** and **49** was to prepare corresponding *N*-methylated phenyl moieties in one (*N*-methylation with methyl iodide) or actually two steps (*O*-demethylation using AlCl_3) as shown in Scheme 11.

2-chloro-4-(methylamino)phenol (**43**) was then treated with the corresponding intermediate (**44** and **1**) produced in the reaction of benzothiazole-2-amine and 6-methoxybenzothiazole-2-amine with CDI (Scheme 12a) to give final products **45** and **46**.



Scheme 11. Synthesis of *N*-methylated aniline derivatives. Reagents and conditions: (a) CH_3I , NaH , THF, 0°C –RT; (b) AlCl_3 , toluene, reflux.



Scheme 12. Synthesis of compound with methylated urea linker. Reagents and conditions: (a) CDI, DCM, RT. (b) amine, MeCN, reflux. (c) CH_3I , NaH , DMF, 0°C –RT; (d) AlCl_3 , toluene, reflux.

Synthesis of final product **49** started with preparation of 3-(benzo[*d*]thiazol-2-yl)-1-(3-chloro-4-methoxyphenyl)-1-methylurea (**47**) from the two previously generated intermediates **42** and **44** (Scheme 12). Compound **47** was then treated with methyl iodide to methylate the other nitrogen on the urea linker (**48**). Finally, *O*-demethylation using AlCl_3 gave the desired product **49** (Scheme 12).

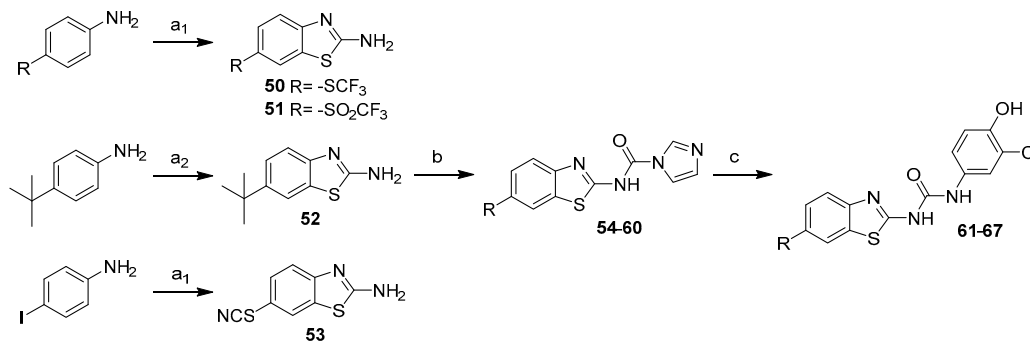
The third series of compounds (Table 3) focused on evaluating substitutions within the benzothiazole ring, predominantly to exploit position 6, a key area highlighted previously [9]. Our previous findings indicated that a 6-trifluoromethoxy moiety and a 6-halogen moiety, led to an increased inhibitory ability towards 17 β -HSD10.

Table 3. Third series of prepared compounds (**61**–**67**).

Compound ID	R
61	<i>i</i> -propyl
62	<i>t</i> -butyl
63	-OEt
64	-SCF ₃
65	-SCN
66	-SO ₂ Me
67	-SO ₂ CF ₃

If not commercially available, the 6-substituted benzothiazole-2-amines were prepared from the corresponding 4-substituted anilines in reaction with potassium isocyanate and

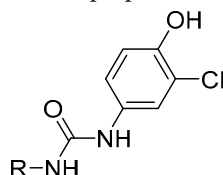
bromine (**50**, **51**) or potassium isocyanate and tetramethylammonium dichloroiodate (**52**). 6-thiocyanatobenzothiazol-2-amine (**53**) was obtained as a by-product during preparation of 6-iodobenzothiazol-2-amine (Scheme 13). The synthesis proceeded according to the general procedure using CDI to give intermediates (**54–60**) and final products **61–67** (Scheme 13).



Scheme 13. Synthesis of 6-substituted benzothiazoles. Reagents and conditions: (a₁) KSCN, Br₂, acetic acid, 10 °C–RT; (a₂) KSCN, tetramethylammonium dichloroiodate, DMSO/water, RT–70 °C; (b) CDI, DCM, RT; (c) 4-amino-2-chlorophenol, MeCN, reflux.

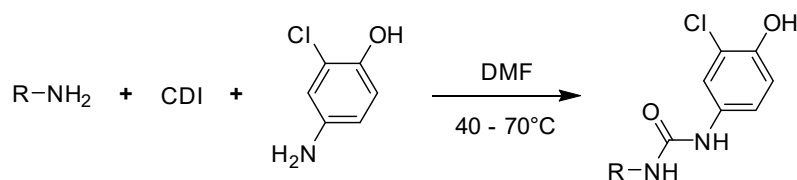
In the fourth series the benzothiazole heterocycle itself became the subject of modifications (as indicated in Table 4). The benzene ring was replaced with a saturated cyclohexane (**71**), separated (**73**) or completely removed (**74**), and the thiazole ring was replaced with an aliphatic cyclopentane (**72**) or replaced with an ethylene bridge (**75**). Further, the whole benzothiazole moiety was flipped and attached to urea via carbon in position 6 of the heterocycle. Moreover, the symmetric derivative (**78**) was prepared to find out whether the dimerized phenyl moiety alone is sufficient for 17β-HSD10 inhibition.

Table 4. Fourth series of prepared compounds (**71–78**).



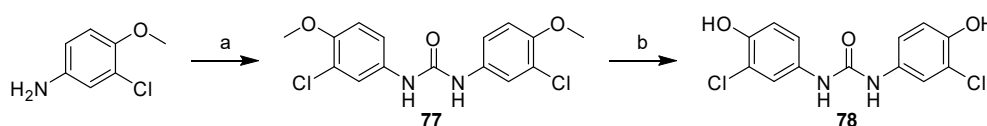
Compound ID	R
71	
72	
73	
74	
75	
76	
78	

The general procedure for synthesis of the urea molecules described earlier in the text (Scheme 1) was only suitable for compounds comprising the 2-aminothiazole core (imidazolecarboxamide intermediates **68–70** and final products **71**, **73** and **74**). Therefore, for compounds **72**, **75** and **76**, the synthesis procedure had to be updated due to an increase in the solubility of imidazolecarboxamide intermediates, which did not allow for their simple isolation by filtration in satisfactory yields. Consequently, after the activation of starting compound with CDI was completed, 4-amino-2-chlorophenol was added directly to the current reaction mixture (Scheme 14).



Scheme 14. One-pot synthesis of phenylureas **72**, **75** and **76**.

The symmetric 1,3-bis(3-chloro-4-hydroxyphenyl)urea (**78**) was prepared in two steps (Scheme 15). First, 3-chloro-4-methoxyaniline was treated with CDI to give 1,3-bis(3-chloro-4-methoxyphenyl)urea (**77**), which was then *O*-demethylated in reaction with AlCl_3 .



Scheme 15. Synthesis of symmetric urea derivative **78**. Reagents and conditions: (a) CDI, DMF, 60 °C; (b) AlCl_3 , toluene, reflux.

2.2. Biochemical and Biophysical Evaluation

In order to reduce attrition rates and improve assay reproducibility we have developed a high throughput screening (HTS) pipeline (Figure 3 [19]). In brief, compounds are screened in the recombinant 17β -HSD10 enzyme activity assay (Table 5, Figure 4). Our best previously published compounds have set the threshold of 40% remaining 17β -HSD10 activity as a minimum standard [9] and if compounds can better this threshold, they are further screened using our orthogonal counter assays, dose response assays and kinetic assessment (Table 5). Finally, if passing these criteria with favourable characteristics, the compounds progress into cellular evaluation through cytotoxicity testing and measuring 17β -HSD10 activity within cells (Table 6).

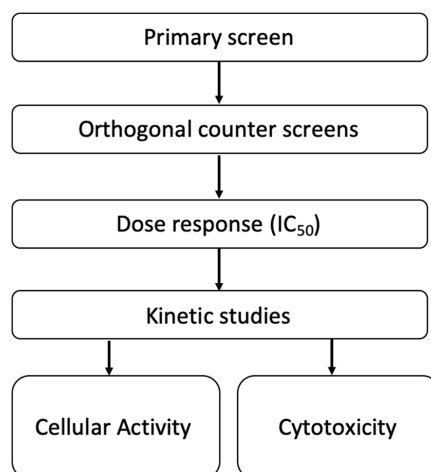


Figure 3. Compound screening pipeline.

Table 5. Biophysical characterisation of compound of interest.

Compound ID	IC ₅₀ Values (μM)	Mechanism of Inhibition with Respect to Both Acetoacetyl-CoA and NADH	Orthogonal Counter Screens: Evidence of Aggregation or Redox Cycling
5	1.28 (95% CI 1.12–1.46)	Mixed	None
6	1.86 (95% CI 1.54–2.26)	Mixed	None
61	5.12 (95% CI 4.61–5.69)	Mixed	None
62	5.29 (95% CI 4.54–6.15)	Mixed	None
63	1.61 (95% CI 1.41–1.83)	Mixed	61% increase in 17β-HSD10 activity within aggregation assay
64	5.21 (95% CI 4.42–6.13)	Mixed	None
65	2.61 (95% CI 2.31–2.94)	Mixed	28.5% increase in 17β-HSD10 activity within aggregation assay
66	0.93 (95% CI 0.82–1.05)	Mixed	None
67	2.69 (95% CI 2.36–3.05)	Mixed	12.6% increase in 17β-HSD10 activity within aggregation assay
78	6.83 (95% CI 5.34–8.75)	Mixed	None

Table 6. Cellular cytotoxicity and potency testing in HEK293 mts17β-HSD10 cells.

Compound ID	(–)-CHANA IC ₅₀ Values (μM)	LDH Cytotoxicity with 100 μM Compound	LDH Cytotoxicity with 25 μM Compound
5	10.39 (95% CI 5.50–19.96)	20.13 ± 4.26	13.28 ± 0.55
6	17.04 (95% CI 9.15–31.73)	23.97 ± 3.32	23.54 ± 3.02
61	7.88 (95% CI 5.07–12.07)	55.68 ± 2.55	28.83 ± 0.67
62	3.77 (95% CI 2.11–6.74)	64.40 ± 3.62	27.25 ± 3.35
63	2.29 (95% CI 1.74–3.01)	18.05 ± 0.96	15.98 ± 1.02
64	-	33.35 ± 2.92	22.83 ± 0.63
65	88.95 (95% CI 28.39–278.7)	27.41 ± 2.65	11.27 ± 0.58
66	-	17.51 ± 0.46	13.59 ± 0.66
67	-	36.05 ± 1.75	22.68 ± 2.68
78	-	12.41 ± 0.64	11.34 ± 0.41

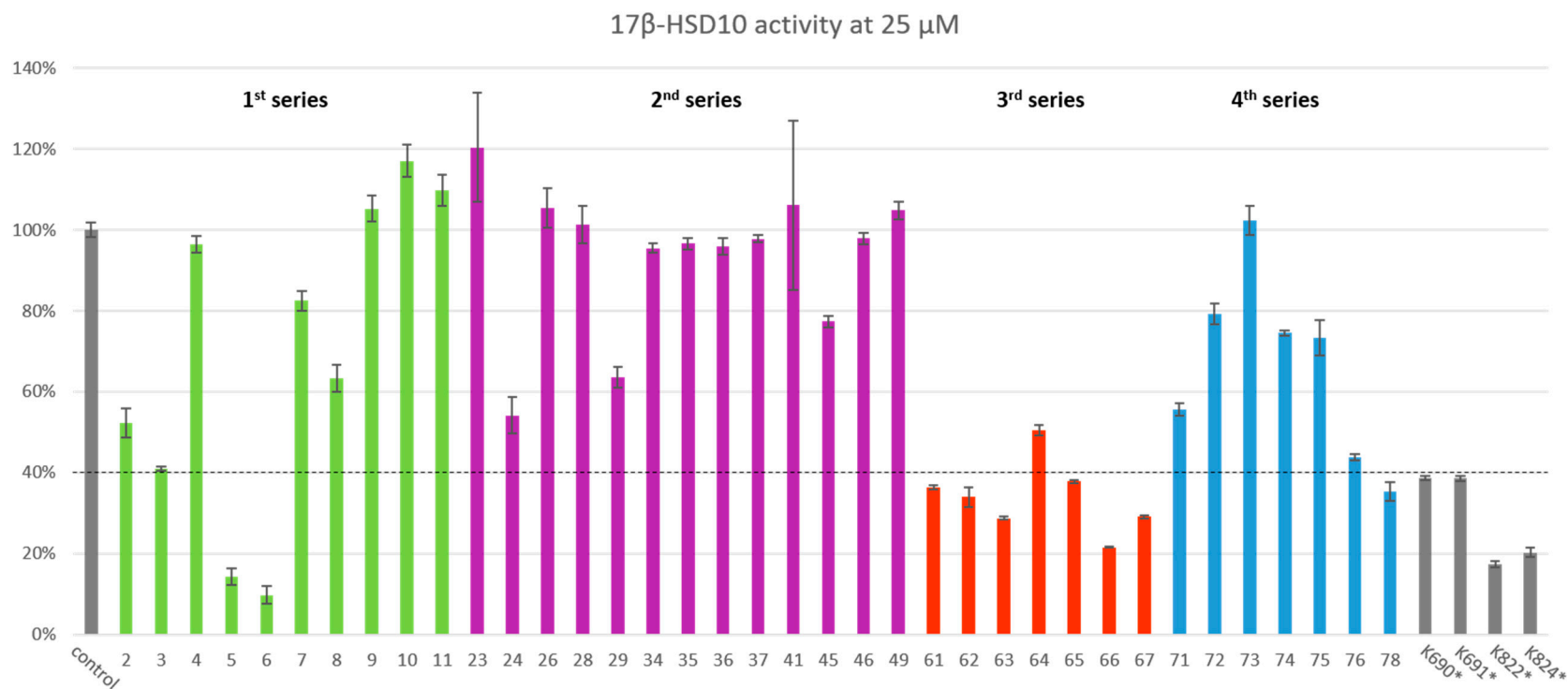


Figure 4. Primary compound in vitro evaluation (relative remaining activity at 25 μ M inhibitor concentration is displayed in percentage of six independent measurements \pm SEM; detailed results in Supplementary data). * Authors' previously published most potent enzymatic data from Hroch et al. 2016 (Design, synthesis and in vitro evaluation of benzothiazole-based ureas as potential ABAD/17 β -HSD10 modulators for Alzheimer's disease treatment) [9].

2.3. Primary Enzyme Assay Results

Full results for the primary nicotinamide adenine dinucleotide (NADH) assay screens are shown in Figure 4 including our four best previously published compounds for comparison (Figure 1) [9].

Our first analogue series (2–11; Table 1 and Figure 4) focused on establishing how alterations to the 3 and 4 position on the distal (phenolic) ring affect inhibition potency. In this series, compounds 5 and 6 showed a huge improvement in potency with remaining 17 β -HSD10 activity of 13.45% and 6.72%, respectively, at 25 μ M. A significant finding from our previous work indicated that a *p*-hydroxy along *m*-chlorine substitution pattern displayed the most pronounced inhibitory activity [9], and a deviation from the 3-halogen and 4-hydroxyl pattern resulted in a dramatic decrease in 17 β -HSD10 inhibition. Our findings in this series further support this, and establish that the bulkier, 3-bromo and 3-iodo substitutions are even more favourable at this position. Replacement of the phenolic hydroxyl with an amine or methylhydroxy group led to loss of activity, which further confirms the importance of the 4-positioned phenolic hydroxyl as was previously suggested [9].

The second analogue series (23–49; Table 2) focused on evaluating changes to the urea linker. Unfortunately, any variation from the urea linker resulted in a dramatic decrease of inhibitory activity (Figure 4). This was further supported by the inclusion of compounds (34–36) previously published by Valasani et al. with the inclusion of our novel phosphonate compound (37) determining that a phosphonate linker did not increase 17 β -HSD10 inhibition. Indeed, all linker variations resulted in negligible changes to 17 β -HSD10 activity with the exception of compound 24. Although the secondary amide substitution (with amide nitrogen attached to benzothiazole moiety) in compound 24 appeared slightly more favourable than most, it was still not as potent as the original urea moiety and just outside of the threshold for further analysis at 47.19% 17 β -HSD10 activity remaining at 25 μ M (Figure 4). Mono and dimethylation of the urea linker to enforce sp³, rather than sp² character, showed a clear detrimental effect on the activity in compound 45–49.

The third series of compounds (61–67) focused on evaluating substitutions within the benzothiazole ring, predominantly to exploit position 6, a key area highlighted previously (Hroch et al. 2016). Our previous findings indicated that a 6-trifluoromethoxy moiety and a 6-halogen moiety led to an increased inhibitory ability towards 17 β -HSD10. This series appear to be the most promising displaying the largest decrease in 17 β -HSD10 activity (indicated in Figure 4), in particular when bulky substitutions at position 6 were applied. This is particularly apparent in compounds 61 and 62 whereby, as the functional group size increases at position 6, 17 β -HSD10 activity decreases with 6-*t*-butyl (62) inhibiting 17 β -HSD10 by 78.36% and the 6-isopropyl substitution (61) inhibiting 17 β -HSD10 by 77.37% at 25 μ M. Other key structure activity relationships in this series have been established through 6-thiol additions (64–67). Again, bulkier substituents produce a larger inhibitory effect with the 6-sulfonyl (66) less effective than the 6-trifluoromethylsulfonyl (67) with 32.16% and 16.16% 17 β -HSD10 activity remaining at 25 μ M. The most potent compound in this series (65) introduced the pseudo-halogenic 6-thiocyanate moiety, which inhibited 17 β -HSD10 activity by 85.69% at 25 μ M.

In order to validate the importance of the benzothiazol-2-yl moiety, several structural analogues were prepared and evaluated in the fourth series (71–78; Table 4). Indeed, any deviation from the benzothiazol-2-yl moiety resulted in decreased biological activity and only the symmetrical compound (78) showed real inhibitory activity with 17 β -HSD10 activity reduced to 40.69% at 25 μ M (Figure 4).

Overall, after primary screening we were left with 10 compounds which would progress down the pipeline: compounds 5, 6, 61, 62, 63, 64, 65, 66, 67 and 78.

2.4. Orthogonal Counter Screens

During our enzymatic assay development, it was noted that the assay was susceptible to false positives through redox cycling and aggregation mechanism [19], therefore, two orthogonal counter screens have been implemented to validate the primary screen results. The addition of the detergent Triton X-100 to the assay buffer prevents the hydrophobic interactions required for aggregation, by which a reduction in inhibition in the presence of Triton X-100 indicates the undesirable inhibitory

mode of action whereby, the compound could be potentially inhibiting the enzyme through the indirect sequestration of the protein. Results (Table 5) identify compound **63** as a potential aggregator as it showed a 61% increase in 17 β -HSD10 activity in the presence of Triton-X100. Compounds **65** and **67** also showed some reduction in activity but this is much less pronounced. Given that these three compounds were part of a small series we decided to advance them into the next step of screening.

With the inclusion of the strong reducing agent dithiothreitol (DTT) in the assay buffer, compounds can appear as a false positive as DTT is capable of generating H₂O₂ causing indirect enzyme inhibition and assay interference. The fluorescence change during the reduction of resazurin to resorufin can be measured as an indication of any redox cycling compounds. The results indicate that none of the compounds appear to be acting via this undesirable mode of action (Table 5).

2.5. Dose Response and Kinetic Evaluation

Our most promising compounds demonstrate reasonable IC₅₀ values of around 1–2 μ M (Table 5 and graphs in Supplementary data). Significantly, these compounds all display a mixed mechanism of inhibition with respect to both substrate acetoacetyl-Coenzyme A and co-factor NADH whereby at low concentrations they appear to act in a competitive manner, but at high concentrations they are inhibiting in other sites (Table 5, Hanes–Wolf plots in Supplementary data). This is favourable over other previously published work [7,20] as the AG18051 compound irreversibly inhibits 17 β -HSD10, forming a covalent adduct with NADH at the active site, thus introducing a potential specificity issue.

2.6. Cellular Screening

Compound toxicity and potency was also assessed using HEK293 mts17 β -HSD10 cells; results are shown in Table 6. Our fluorogenic probe, (–)-CHANA, a 17 β -HSD10 substrate [21] was used to calculate cellular IC₅₀ values (graphs in Supplementary data) with the exception of compounds **64**, **66**, **67** and **78**, which were precipitating within the assay media and not able to effectively penetrate into cells. Compounds **61**, **62** and **63** proved to be the most potent in our cellular assay with IC₅₀ values of 7.88, 3.77 and 2.29 μ M, respectively.

Lactate dehydrogenase (LDH) is a colorimetric assay routinely used to quantitatively measure LDH released into the media from damaged cells as a biomarker for cellular cytotoxicity and cytolysis. HEK293 mts17 β -HSD10 cells were treated with compound (100 and 25 μ M) for 24 h before measurements were taken. At 25 μ M compounds showed around 10–30% cytotoxicity, however, this concentration is substantially higher than the measured IC₅₀ values and as such is not a cause for concern. Compound **65** showed a remarkably higher IC₅₀ value in the (–)-CHANA assay which suggests that the uptake of compound by cells and 17 β -HSD10 target engagement is not as favourable as others.

3. Materials and Methods

3.1. General Chemistry

All reagents and solvents were purchased from commercial sources (Sigma Aldrich, Prague, Czech Republic; Activate Scientific, Prien, Germany; Alfa Aesar, Kandel, Germany; Merck, Darmstadt, Germany; Penta Chemicals, Prague, Czech Republic and VWR, Stribrna Skalice, Czech Republic) and they were used without any further purification. Low boiling point ($\geq 90\%$ 40–60 °C) petroleum ether (PE) was used if not stated otherwise.

Thin-layer chromatography (TLC) for reaction monitoring was performed on Merck aluminium sheets, silica gel 60 F₂₅₄ (Darmstadt, Germany). Visualisation was performed either via UV (254 nm) or appropriate stain reagent solutions (alternatively in combination of both). Preparative column chromatography was performed on silica gel 60 (70–230 mesh, 63–200 μ m, 60 Å pore size). Melting points were determined on a Stuart SMP30 melting point apparatus and are uncorrected.

Nuclear magnetic resonance (NMR) spectra were acquired at 500/126/202 MHz (^1H , ^{13}C and ^{31}P) on a Varian S500 spectrometer or at 300/75 MHz (^1H and ^{13}C) on a Varian Gemini 300 spectrometer (both produced by Palo Alto, CA, USA). Chemical shifts δ are given in ppm and referenced to the signal center of solvent peaks (DMSO- d_6 : δ 2.50 ppm and 39.52 ppm for ^1H and ^{13}C , respectively; Chloroform- d : δ 7.26 ppm and 77.16 ppm for ^1H and ^{13}C , respectively), thus indirectly correlated to TMS standard (δ 0 ppm). Chemical shifts δ for ^{31}P are given in ppm and referenced to the phosphoric acid standard (δ 0 ppm). Coupling constants are expressed in Hz.

High-resolution mass spectra (HRMS) were recorded by coupled LC-MS system consisting of Dionex UltiMate 3000 analytical LC system and Q Exactive Plus hybrid quadrupole-orbitrap spectrometer (both produced by ThermoFisher Scientific, Bremen, Germany). As an ion-source, heated electro-spray ionization (HESI) was utilised (setting: sheath gas flow rate 40, aux gas flow rate 10, sweep gas flow rate 2, spray voltage 3.2 kV, capillary temperature 350 °C, aux gas temperature 300 °C, S-lens RF level 50). Positive ions were monitored in the range of 100–1500 m/z with the resolution set to 140,000. Obtained mass spectra were processed in Xcalibur 3.0.63 software (ThermoFisher Scientific, Bremen, Germany).

Further synthetic information can be found in the Supplementary material.

3.2. Final Products Characterization

The purification method is specified here only when altered from the generally used method described in Supplementary information.

1-(4-Hydroxy-3-methylphenyl)-3-(6-methoxybenzo[d]thiazol-2-yl)urea (2) Yield 85%; mp: 262–263 °C; $^1\text{H-NMR}$ (500 MHz, DMSO- d_6): δ (ppm) 10.55 (br s, 1H), 9.09 (s, 1H), 8.77 (s, 1H), 7.54 (d, J = 8.8 Hz, 1H), 7.50 (d, J = 2.6 Hz, 1H), 7.18 (d, J = 2.6 Hz, 1H), 7.10 (dd, J = 8.5, 2.7 Hz, 1H), 6.97 (dd, J = 8.8, 2.6 Hz, 1H), 6.73 (d, J = 8.5 Hz, 1H), 3.79 (s, 3H), 2.12 (s, 3H); $^{13}\text{C-NMR}$ (126 MHz, DMSO- d_6): δ (ppm) 157.57, 155.61, 151.75, 151.47, 142.84, 132.53, 129.56, 124.11, 122.24, 120.13, 118.18, 114.64, 114.29, 104.87, 55.60, 16.12; HRMS (ESI) calcd for $\text{C}_{16}\text{H}_{16}\text{N}_3\text{O}_3\text{S}$ [$\text{M} + \text{H}$] $^+$ 330.09069, found 330.09039.

1-(3-(Tert-butyl)-4-hydroxyphenyl)-3-(6-methoxybenzo[d]thiazol-2-yl)urea (3) Yield 73%; mp: 259–260 °C; $^1\text{H-NMR}$ (500 MHz, DMSO- d_6): δ (ppm) 10.47 (br s, 1H), 9.18 (br s, 1H), 8.79 (s, 1H), 7.54 (d, J = 8.8 Hz, 1H), 7.49 (d, J = 2.6 Hz, 1H), 7.19 (d, J = 2.6 Hz, 1H), 7.17 (dd, J = 8.4, 2.6 Hz, 1H), 6.97 (dd, J = 8.8, 2.6 Hz, 1H), 6.73 (d, J = 8.4 Hz, 1H), 3.79 (s, 3H), 1.35 (s, 9H); $^{13}\text{C-NMR}$ (126 MHz, DMSO- d_6): δ (ppm) 157.50, 155.61, 151.91, 151.84, 142.82, 135.53, 132.60, 129.43, 120.20, 118.58, 118.38, 116.13, 114.28, 104.90, 55.62, 34.35, 29.25; HRMS (ESI) calcd for $\text{C}_{19}\text{H}_{22}\text{N}_3\text{O}_3\text{S}$ [$\text{M} + \text{H}$] $^+$ 372.13764, found 372.13730.

1-(3-Cyano-4-hydroxyphenyl)-3-(6-methoxybenzo[d]thiazol-2-yl)urea (4) Yield 98%; mp: 277–279 °C; $^1\text{H-NMR}$ (500 MHz, DMSO- d_6): δ (ppm) 10.86 (s, 1H), 9.37 (s, 1H), 7.76 (d, J = 2.7 Hz, 1H), 7.56–7.52 (m, 2H), 7.51 (d, J = 2.6 Hz, 1H), 7.01 (d, J = 9.0 Hz, 1H), 6.98 (dd, J = 8.8, 2.6 Hz, 1H), 3.79 (s, 3H); $^{13}\text{C-NMR}$ (126 MHz, DMSO- d_6): δ (ppm) 157.84, 156.05, 155.71, 152.44, 141.78, 132.24, 130.54, 126.52, 122.87, 119.79, 116.80, 116.73, 114.40, 105.00, 98.49, 55.61; HRMS (ESI) calcd for $\text{C}_{16}\text{H}_{12}\text{N}_4\text{O}_3\text{S}$ [$\text{M} + \text{H}$] $^+$ 341.07029, found 341.07016.

1-(3-Bromo-4-hydroxyphenyl)-3-(6-methoxybenzo[d]thiazol-2-yl)urea (5) Yield 82%; mp: 246–247 °C; $^1\text{H-NMR}$ (500 MHz, DMSO- d_6): δ (ppm) 10.71 (br s, 1H), 9.99 (s, 1H), 8.97 (s, 1H), 7.75 (s, 1H), 7.54 (d, J = 8.4 Hz, 1H), 7.50 (s, 1H), 7.22 (d, J = 8.6 Hz, 1H), 6.97 (d, J = 8.5 Hz, 1H), 6.92 (d, J = 8.6 Hz, 1H), 3.79 (s, 3H); $^{13}\text{C-NMR}$ (126 MHz, DMSO- d_6): δ (ppm) 157.84, 155.67, 152.21, 149.97, 142.25, 132.33, 131.04, 123.65, 120.14, 119.87, 116.28, 114.37, 108.86, 104.95, 55.61; HRMS (ESI) calcd for $\text{C}_{15}\text{H}_{13}\text{BrN}_3\text{O}_3\text{S}$ [$\text{M} + \text{H}$] $^+$ 393.98555, found 393.98489.

1-(4-Hydroxy-3-iodophenyl)-3-(6-methoxybenzo[d]thiazol-2-yl)urea (6) Yield 85%; mp: 241–242 °C; $^1\text{H-NMR}$ (300 MHz, DMSO- d_6): δ (ppm) 10.07 (br s, 1H), 9.05 (s, 1H), 7.90 (d, J = 2.6 Hz, 1H), 7.54 (d, J = 8.8 Hz, 1H), 7.51 (d, J = 2.6 Hz, 1H), 7.25 (dd, J = 8.7, 2.6 Hz, 1H), 6.97 (dd, J = 8.8, 2.6 Hz, 1H), 6.85 (d, J = 8.7 Hz, 1H), 3.79 (s, 3H); $^{13}\text{C-NMR}$ (75 MHz, DMSO- d_6): δ (ppm) 157.72, 155.67, 152.67, 152.10, 142.15, 132.35,

131.29, 129.42, 120.99, 119.93, 114.75, 114.38, 104.93, 84.10, 55.62; HRMS (ESI) calcd for $C_{15}H_{13}IN_3O_3S$ $[M + H]^+$ 441.97168, found 441.97049.

1-(3-Amino-4-hydroxyphenyl)-3-(6-methoxybenzo[d]thiazol-2-yl)urea (7) Yield 53%; mp: 180–181 °C; 1H -NMR (500 MHz, DMSO- d_6): δ (ppm) 10.41 (br s, 1H), 8.76 (br s, 1H), 8.65 (s, 1H), 7.53 (d, $J = 8.8$ Hz, 1H), 7.49 (d, $J = 2.6$ Hz, 1H), 6.96 (dd, $J = 8.8, 2.6$ Hz, 1H), 6.82 (d, $J = 2.6$ Hz, 1H), 6.57 (d, $J = 8.3$ Hz, 1H), 6.47 (dd, $J = 8.3, 2.5$ Hz, 1H), 4.61 (s, 2H), 3.79 (s, 3H); ^{13}C -NMR (126 MHz, DMSO- d_6): δ (ppm) 157.45, 155.57, 151.34, 143.00, 140.11, 136.90, 132.57, 130.42, 122.10, 120.22, 114.24, 107.26, 106.17, 104.84, 55.58; HRMS (ESI) calcd for $C_{15}H_{15}N_4O_3S$ $[M + H]^+$ 331.08594, found 331.08527.

1-(6-Hydroxypyridin-3-yl)-3-(6-methoxybenzo[d]thiazol-2-yl)urea (8) Yield 82%; mp: 272–273 °C; 1H -NMR (300 MHz, DMSO- d_6): δ (ppm) 11.38 (br s, 1H), 9.08 (br s, 1H), 7.64 (s, 1H), 7.59 (d, $J = 9.1$ Hz, 1H), 7.53–7.39 (m, 2H), 6.97 (dd, $J = 9.2, 2.6$ Hz, 1H), 6.36 (d, $J = 10.1$ Hz, 1H), 3.79 (s, 3H); ^{13}C -NMR (75 MHz, DMSO- d_6): δ (ppm) 160.85, 158.50, 155.83, 153.21, 142.19, 138.04, 132.42, 127.92, 120.11, 119.28, 119.17, 114.49, 105.11, 55.78; HRMS (ESI) calcd for $C_{14}H_{13}N_4O_3S$ $[M + H]^+$ 317.07029, found 317.07004.

1-(4-Aminophenyl)-3-(6-methoxybenzo[d]thiazol-2-yl)urea (9) Yield 93%; mp: 304–306 °C (decomp); 1H -NMR (500 MHz, DMSO- d_6): δ (ppm) 10.46 (br s, 1H), 8.63 (s, 1H), 7.54 (d, $J = 8.8$ Hz, 1H), 7.50 (d, $J = 2.6$ Hz, 1H), 7.15–7.10 (m, 2H), 6.96 (dd, $J = 8.8, 2.6$ Hz, 1H), 6.57–6.52 (m, 2H), 4.90 (s, 2H), 3.79 (s, 3H); ^{13}C -NMR (126 MHz, DMSO- d_6): δ (ppm) 157.58, 155.56, 151.75, 144.96, 142.74, 132.56, 127.01, 121.23, 120.12, 114.23, 114.05, 104.87, 55.58; HRMS (ESI) calcd for $C_{15}H_{15}N_4O_2S$ $[M + H]^+$ 315.09102, found 315.09058.

1-(4-Amino-3-chlorophenyl)-3-(6-methoxybenzo[d]thiazol-2-yl)urea (10) Yield 78%; mp: 310–311 °C (decomp); 1H -NMR (500 MHz, DMSO- d_6): δ (ppm) 10.60 (br s, 1H), 8.82 (s, 1H), 7.54 (d, $J = 8.7$ Hz, 1H), 7.50 (d, $J = 2.6$ Hz, 1H), 7.47 (d, $J = 2.4$ Hz, 1H), 7.06 (dd, $J = 8.6, 2.4$ Hz, 1H), 6.97 (dd, $J = 8.8, 2.6$ Hz, 1H), 6.78 (d, $J = 8.6$ Hz, 1H), 5.14 (s, 2H), 3.79 (s, 3H); ^{13}C -NMR (126 MHz, DMSO- d_6): δ (ppm) 157.69, 155.61, 151.90, 140.78, 132.42, 128.05, 120.50, 120.23, 119.97, 116.77, 115.48, 114.29, 104.91, 55.59; HRMS (ESI) calcd for $C_{15}H_{14}ClN_4O_2S$ $[M + H]^+$ 349.05205, found 349.05154.

1-(3-Chloro-4-(hydroxymethyl)phenyl)-3-(6-methoxybenzo[d]thiazol-2-yl)urea (11) Yield 92%; mp: 229–230 °C; 1H -NMR (500 MHz, DMSO- d_6): δ (ppm) 10.84 (br s, 1H), 9.26 (s, 1H), 7.72 (d, $J = 2.2$ Hz, 1H), 7.55 (d, $J = 8.7$ Hz, 1H), 7.51 (d, $J = 2.6$ Hz, 1H), 7.47 (d, $J = 8.4$ Hz, 1H), 7.38 (dd, $J = 8.4$ Hz, 2.1 Hz, 1H), 6.98 (dd, $J = 8.8, 2.6$ Hz, 1H), 5.29 (t, $J = 5.6$ Hz, 1H), 4.53 (d, $J = 5.2$ Hz, 2H), 3.80 (s, 3H); ^{13}C -NMR (126 MHz, DMSO- d_6): δ (ppm) 157.75, 155.74, 152.27, 138.45, 133.63, 132.18, 131.19, 128.67, 127.18, 119.85, 118.56, 117.35, 114.44, 105.01, 59.99, 55.61; HRMS (ESI) calcd for $C_{16}H_{15}ClN_3O_3S$ $[M + H]^+$ 364.05172, found 364.05103.

2-Chloro-4-((6-chlorobenzo[d]thiazol-2-yl)amino)phenol (23) Yield 30%; mp: 213–214.5 °C; 1H -NMR (500 MHz, DMSO- d_6): δ (ppm) 10.49 (br s, 1H), 9.92 (br s, 1H), 7.94–7.85 (m, 2H), 7.54 (d, $J = 8.6$ Hz, 1H), 7.40 (dd, $J = 8.8, 2.6$ Hz, 1H), 7.31 (dd, $J = 8.6, 2.2$ Hz, 1H), 6.98 (d, $J = 8.8$ Hz, 1H); ^{13}C -NMR (126 MHz, DMSO- d_6): δ (ppm) 162.53, 150.83, 148.56, 132.94, 131.53, 126.01, 125.88, 120.74, 119.86, 119.74, 119.43, 118.46, 116.87; HRMS (ESI) calcd for $C_{13}H_8Cl_2N_2OS$ $[M + H]^+$ 310.98072, found 310.98016.

3-Chloro-4-hydroxy-N-(6-methoxybenzo[d]thiazol-2-yl)benzamide (24) Yield 69%; mp: 301.5–302.5 °C; 1H -NMR (300 MHz, DMSO- d_6): δ (ppm) 12.51 (br s, 1H), 11.25 (br s, 1H), 8.21 (s, 1H), 7.97 (d, $J = 8.6$ Hz, 1H), 7.66 (d, $J = 8.9$ Hz, 1H), 7.59 (s, 1H), 7.17–6.96 (m, 2H), 3.82 (s, 3H); ^{13}C -NMR (75 MHz, DMSO- d_6): δ (ppm) 164.08, 157.27, 156.85, 156.21, 142.57, 132.85, 130.34, 128.93, 123.50, 120.96, 119.89, 116.34, 115.00, 104.66, 55.64; HRMS (ESI) calcd for $C_{15}H_{11}ClN_2O_3S$ $[M + H]^+$ 335.02517, found 335.02466.

N-(3-Chloro-4-hydroxyphenyl)-6-methoxybenzo[d]thiazole-2-carboxamide (26) Yield 58%; mp: 260–261.5 °C; 1H -NMR (500 MHz, DMSO- d_6): δ (ppm) 10.94 (br s, 1H), 10.09 (br s, 1H), 8.06 (d, $J = 8.4$ Hz, 1H), 7.94 (s, 1H), 7.80 (s, 1H), 7.65 (d, $J = 7.7$ Hz, 1H), 7.23 (d, $J = 8.1$ Hz, 1H), 6.97 (d, $J = 8.2$ Hz, 1H), 3.88 (s, 3H); ^{13}C -NMR (126 MHz, DMSO- d_6): δ (ppm) 161.76, 158.62, 157.88, 149.87, 147.05, 138.22, 130.34, 124.71,

122.22, 120.81, 119.09, 117.30, 116.36, 104.79, 55.84; HRMS (ESI) calcd for $C_{15}H_{11}ClN_2O_3S [M + H]^+$ 335.02517, found 335.02466.

1-(3-Chloro-4-hydroxybenzyl)-3-(6-methoxybenzo[d]thiazol-2-yl)urea (28)

The crude product was purified using column chromatography.

Yield 20%; mp: 249–251 °C; 1H -NMR (500 MHz, DMSO- d_6): δ (ppm) 10.60 (br s, 1H), 10.08 (br s, 1H), 7.51 (d, $J = 8.8$ Hz, 1H), 7.48 (d, $J = 2.6$ Hz, 1H), 7.29 (d, $J = 2.1$ Hz, 1H), 7.13 (t, $J = 5.3$ Hz, 1H), 7.10 (dd, $J = 8.3, 2.1$ Hz, 1H), 6.98–6.90 (m, 2H), 4.25 (d, $J = 5.9$ Hz, 2H), 3.78 (s, 3H); ^{13}C -NMR (126 MHz, DMSO- d_6): δ (ppm) 157.80, 155.52, 153.84, 152.01, 143.16, 132.59, 131.25, 128.80, 127.18, 120.19, 119.37, 116.54, 114.15, 104.81, 55.57, 42.01; HRMS (ESI) calcd for $C_{16}H_{14}ClN_3O_3S [M + H]^+$ 364.05172, found 364.05115.

1-(3,4-Dihydroxybenzyl)-3-(6-methoxybenzo[d]thiazol-2-yl)urea (29)

After the reaction was completed (monitored by TLC), 1M aq. HCl was poured to the reaction mixture and the product was extracted to DCM. The organic layer was concentrated and the crude product was recrystallized from MeCN.

Yield 50%; mp: 141.5–142 °C; 1H -NMR (500 MHz, DMSO- d_6): δ (ppm) 7.51 (d, $J = 8.8$ Hz, 1H), 7.48 (d, $J = 2.6$ Hz, 1H), 7.15 (br s, 1H), 6.95 (dd, $J = 8.8, 2.6$ Hz, 1H), 6.71 (d, $J = 2.0$ Hz, 1H), 6.68 (d, $J = 8.0$ Hz, 1H), 6.56 (dd, $J = 8.0, 2.0$ Hz, 1H), 4.18 (d, $J = 5.5$ Hz, 2H), 3.78 (s, 3H); ^{13}C -NMR (126 MHz, DMSO- d_6): δ (ppm) 158.51, 155.74, 153.64, 145.23, 144.41, 141.36, 131.95, 129.93, 119.61, 118.26, 115.49, 114.93, 114.45, 105.07, 55.65, 42.68; HRMS (ESI) calcd for $C_{16}H_{15}N_3O_4S [M + H]^+$ 346.08560, found 346.08517.

Dimethyl ((4-fluorophenyl)((6-methoxybenzo[d]thiazol-2-yl)amino)methyl) phosphonate (34) (Valasani et al. 2013). Yield 65%; mp: 173–174 °C; 1H -NMR (500 MHz, DMSO- d_6): δ (ppm) 9.48 (s, 1H), 8.76 (dd, $J = 9.7, 2.9$ Hz, 1H), 7.33–7.27 (m, 4H), 6.82 (dd, $J = 8.7, 2.7$ Hz, 1H), 6.75 (d, $J = 8.4$ Hz, 2H), 5.54 (dd, $J = 20.9, 9.7$ Hz, 1H), 3.72 (s, 3H), 3.64 (d, $J = 10.5$ Hz, 3H), 3.50 (d, $J = 10.5$ Hz, 3H); ^{13}C -NMR (126 MHz, DMSO- d_6): δ (ppm) 163.62 (d, $J = 10.0$ Hz), 161.69 (dd, $J = 244.1, 2.9$ Hz), 154.67, 145.52, 132.10 (d, $J = 2.9$ Hz), 131.87, 130.02 (dd, $J = 8.3, 5.5$ Hz), 118.79, 115.18 (dd, $J = 21.6, 1.7$ Hz), 113.09, 105.58, 53.53 (d, $J = 6.8$ Hz), 53.25 (d, $J = 6.8$ Hz), 53.12 (d, $J = 154.1$ Hz); ^{31}P NMR (202 MHz, DMSO- d_6): δ (ppm) 23.56 (d, $J = 4.5$ Hz); HRMS (ESI) calcd for $C_{17}H_{19}FN_2O_4PS [M + H]^+$ 397.07817, found 397.07755.

Dimethyl ((4-hydroxyphenyl)((6-methoxybenzo[d]thiazol-2-yl)amino)methyl) phosphonate (35) (Valasani et al. 2013). Yield 76%; mp: 217–218 °C; 1H -NMR (500 MHz, DMSO- d_6): δ (ppm) 9.48 (s, 1H), 8.76 (dd, $J = 9.7, 2.9$ Hz, 1H), 7.33–7.28 (m, 4H), 6.82 (dd, $J = 8.7, 2.7$ Hz, 1H), 6.75 (d, $J = 8.4$ Hz, 2H), 5.54 (dd, $J = 20.9, 9.7$ Hz, 1H), 3.72 (s, 3H), 3.64 (d, $J = 10.5$ Hz, 3H), 3.50 (d, $J = 10.5$ Hz, 3H); ^{13}C -NMR (126 MHz, DMSO- d_6): δ (ppm) 163.70 (d, $J = 10.0$ Hz), 157.06 (d, $J = 2.4$ Hz), 154.57, 145.64, 131.82, 129.31 (d, $J = 5.7$ Hz), 125.77, 118.68, 115.08, 113.01, 105.57, 55.53, 53.33 (d, $J = 6.9$ Hz), 53.28 (d, $J = 155.2$ Hz), 53.14 (d, $J = 6.9$ Hz); ^{31}P NMR (202 MHz, DMSO- d_6): δ (ppm) 24.25; HRMS (ESI) calcd for $C_{17}H_{20}N_2O_5PS [M + H]^+$ 395.08251, found 395.08215.

Methyl 5-((dimethoxyphosphoryl)((6-methoxybenzo[d]thiazol-2-yl)amino)methyl)-2-hydroxybenzoate (36) (Valasani et al. 2013) Yield 73%; mp: 180–181 °C; 1H -NMR (500 MHz, DMSO- d_6): δ (ppm) 10.53 (s, 1H), 8.90 (dd, $J = 9.6, 3.5$ Hz, 1H), 7.95 (t, $J = 2.3$ Hz, 1H), 7.65 (dt, $J = 8.7, 2.1$ Hz, 1H), 7.32 (d, $J = 2.7$ Hz, 1H), 7.30 (d, $J = 8.7$ Hz, 1H), 7.01 (d, $J = 8.6$ Hz, 1H), 6.82 (dd, $J = 8.8, 2.7$ Hz, 1H), 5.63 (dd, $J = 21.3, 9.4$ Hz, 1H), 3.91 (s, 3H), 3.72 (s, 3H), 3.67 (d, $J = 10.6$ Hz, 3H), 3.55 (d, $J = 10.6$ Hz, 3H); ^{13}C -NMR (126 MHz, DMSO- d_6): δ (ppm) 168.86, 163.61 (d, $J = 10.1$ Hz), 159.53 (d, $J = 2.0$ Hz), 154.65, 145.52, 135.35 (d, $J = 5.1$ Hz), 131.88, 129.33 (d, $J = 6.0$ Hz), 126.83, 118.79, 117.49, 105.58, 113.07, 113.03 (d, $J = 1.9$ Hz), 55.53, 53.55 (d, $J = 7.1$ Hz), 53.26 (d, $J = 6.8$ Hz), 52.90 (d, $J = 155.2$ Hz), 52.53; ^{31}P NMR (202 MHz, DMSO- d_6): δ (ppm) 23.67; HRMS (ESI) calcd for $C_{19}H_{22}N_2O_7PS [M + H]^+$ 453.08798, found 453.08701.

Dimethyl ((3-chloro-4-hydroxyphenyl)((6-methoxybenzo[d]thiazol-2-yl)amino)methyl) phosphonate (37) Yield 65%; mp: 198–199 °C; 1H -NMR (500 MHz, DMSO- d_6): δ (ppm) 10.28 (s, 1H), 8.77 (dd, $J = 9.7, 3.1$ Hz,

1H), 7.50 (t, $J = 2.1$ Hz, 1H), 7.32 (d, $J = 2.7$ Hz, 1H), 7.31 (d, $J = 8.8$ Hz, 1H), 7.27 (dt, $J = 8.5, 2.1$ Hz, 1H), 6.95 (d, $J = 8.4$ Hz, 1H), 6.82 (dd, $J = 8.7, 2.6$ Hz, 1H), 5.57 (dd, $J = 21.0, 9.6$ Hz, 1H), 3.73 (s, 3H), 3.66 (d, $J = 10.6$ Hz, 3H), 3.55 (d, $J = 10.6$ Hz, 3H); ^{13}C -NMR (126 MHz, DMSO- d_6): δ (ppm) 163.76 (d, $J = 10.1$ Hz), 154.82, 152.90 (d, $J = 2.4$ Hz), 145.72, 132.01, 129.40 (d, $J = 5.4$ Hz), 128.12 (d, $J = 5.9$ Hz), 127.58, 119.66 (d, $J = 2.2$ Hz), 118.94, 116.52, 113.25, 105.76, 55.71, 53.66 (d, $J = 6.8$ Hz), 53.41 (d, $J = 7.0$ Hz), 52.95 (d, $J = 155.3$ Hz); ^{31}P NMR (202 MHz, DMSO- d_6): δ (ppm) 23.71; HRMS (ESI) calcd for $\text{C}_{17}\text{H}_{19}\text{ClN}_2\text{O}_5\text{PS}$ $[\text{M} + \text{H}]^+$ 429.04353, found 429.0425.

1-(Benzo[d]thiazol-2-yl)-3-(3-chloro-4-hydroxyphenyl)-1-methylurea (41) Yield 83%; mp: 171–172 °C; ^1H -NMR (500 MHz, DMSO- d_6): δ (ppm) 10.02 (s, 1H), 9.47 (s, 1H), 7.94 – 7.84 (m, 1H), 7.74 (d, $J = 7.9$ Hz, 1H), 7.57 (d, $J = 2.6$ Hz, 1H), 7.45 – 7.35 (m, 1H), 7.31 (dd, $J = 8.8, 2.6$ Hz, 1H), 7.28 – 7.19 (m, 1H), 6.96 (d, $J = 8.7$ Hz, 1H), 3.75 (s, 3H); ^{13}C -NMR (126 MHz, DMSO- d_6): δ (ppm) 161.45, 153.45, 149.66, 148.45, 132.76, 130.50, 125.80, 123.42, 123.09, 121.95, 121.12, 120.29, 119.01, 116.29, 34.55 (d, $J = 3.0$ Hz); HRMS (ESI) calcd for $\text{C}_{15}\text{H}_{12}\text{ClN}_3\text{O}_2\text{S}$ $[\text{M} + \text{H}]^+$ 334.04115, found 334.04080.

3-(Benzo[d]thiazol-2-yl)-1-(3-chloro-4-hydroxyphenyl)-1-methylurea (45)

The crude product was dissolved in Et_2O and filtered. To the filtrate was added PE and the solution was left to crystallize in a freezer. Filtration gave the desired pure product.

Yield 53%; mp: 139–141 °C; ^1H -NMR (500 MHz, DMSO- d_6): δ (ppm) 10.28 (br s, 1H), 7.81 (d, $J = 7.5$ Hz, 1H), 7.45 (br s, 1H), 7.38 – 7.30 (m, 2H), 7.19 (t, $J = 7.9$ Hz, 1H), 7.11 (dd, $J = 8.6, 2.5$ Hz, 1H), 6.99 (d, $J = 8.6$ Hz, 1H), 3.26 (s, 3H); ^{13}C -NMR (126 MHz, DMSO- d_6): δ (ppm) 151.90, 135.11, 128.70, 126.89, 125.94, 122.65, 121.62, 119.46, 116.66, 37.93; HRMS (ESI) calcd for $\text{C}_{15}\text{H}_{12}\text{ClN}_3\text{O}_2\text{S}$ $[\text{M} + \text{H}]^+$ 334.0412, found 334.0414.

1-(3-Chloro-4-hydroxyphenyl)-3-(6-methoxybenzo[d]thiazol-2-yl)-1-methylurea (46)

The crude product was purified using column chromatography.

Yield 50%; mp: 220 °C decomp.; ^1H -NMR (500 MHz, DMSO- d_6): δ (ppm) 10.28 (br s, 1H), 7.45 (d, $J = 2.2$ Hz, 1H), 7.38 (d, $J = 8.1$ Hz, 1H), 7.36 (d, $J = 2.5$ Hz, 1H), 7.11 (dd, $J = 8.6, 2.5$ Hz, 1H), 6.98 (d, $J = 8.6$ Hz, 1H), 6.94 (dd, $J = 8.8, 2.6$ Hz, 1H), 3.77 (s, 3H), 3.25 (s, 3H); ^{13}C -NMR (126 MHz, DMSO- d_6): δ (ppm) 155.57, 151.97, 134.94, 131.53, 128.78, 126.95, 119.52, 118.40, 116.70, 114.18, 105.12, 55.60, 37.94; HRMS (ESI) calcd for $\text{C}_{16}\text{H}_{14}\text{ClN}_3\text{O}_3\text{S}$ $[\text{M} + \text{H}]^+$ 364.0517, found 364.0530.

1-(Benzo[d]thiazol-2-yl)-3-(3-chloro-4-hydroxyphenyl)-1,3-dimethylurea (49) Yield 65%; mp: 227–228.5 °C; ^1H -NMR (500 MHz, DMSO- d_6): δ (ppm) 10.09 (s, 1H), 7.74 (d, $J = 7.7$ Hz, 1H), 7.47 – 7.37 (m, 2H), 7.36 (d, $J = 2.4$ Hz, 1H), 7.23 (t, $J = 7.9$ Hz, 1H), 7.13 (dd, $J = 8.6, 2.2$ Hz, 1H), 6.95 (d, $J = 8.7$ Hz, 1H); ^{13}C -NMR (126 MHz, DMSO- d_6): δ (ppm) 165.20, 160.92, 150.53, 137.50, 136.58, 127.60, 126.56, 125.93, 125.38, 123.01, 122.40, 118.67, 115.86, 111.35, 37.16, 31.51; HRMS (ESI) calcd for $\text{C}_{16}\text{H}_{14}\text{ClN}_3\text{O}_2\text{S}$ $[\text{M} + \text{H}]^+$ 348.05680, found 348.05661.

1-(3-Chloro-4-hydroxyphenyl)-3-(6-isopropylbenzo[d]thiazol-2-yl)urea (61) Yield 43%; mp: 246–248 °C; ^1H -NMR (500 MHz, DMSO- d_6): δ (ppm) 10.83 (br s, 1H), 9.91 (br s, 1H), 9.02 (s, 1H), 7.74 (s, 1H), 7.61 (d, $J = 2.4$ Hz, 1H), 7.54 (d, $J = 8.2$ Hz, 1H), 7.26 (dd, $J = 8.3, 1.5$ Hz, 1H), 7.19 (dd, $J = 8.7, 2.4$ Hz, 1H), 6.93 (d, $J = 8.7$ Hz, 1H), 6.73 (d, $J = 8.7$ Hz, 1H), 2.97 (sept, $J = 6.9$ Hz, 1H), 1.23 (d, $J = 6.9$ Hz, 6H); ^{13}C -NMR (126 MHz, DMSO- d_6): δ (ppm) 159.33, 152.47, 148.89, 146.08, 143.46, 131.02, 130.84, 124.67, 120.74, 119.41, 119.33, 118.68, 116.64, 33.41, 24.17; HRMS (ESI) calcd for $\text{C}_{17}\text{H}_{16}\text{ClN}_3\text{O}_2\text{S}$ $[\text{M} + \text{H}]^+$ 362.0725, found 362.0721.

1-(6-(Tert-butyl)benzo[d]thiazol-2-yl)-3-(3-chloro-4-hydroxyphenyl)urea (62) Yield 66%; mp: 238–240 °C; ^1H -NMR (500 MHz, DMSO- d_6): δ (ppm) 9.75 (s, 1H), 7.90 (d, $J = 1.9$ Hz, 1H), 7.60 (d, $J = 2.6$ Hz, 1H), 7.56 (d, $J = 8.5$ Hz, 1H), 7.43 (dd, $J = 8.5, 2.0$ Hz, 1H), 7.18 (dd, $J = 8.8, 2.6$ Hz, 1H), 6.95 (d, $J = 8.7$ Hz, 1H), 1.32 (s, 9H); ^{13}C -NMR (126 MHz, DMSO- d_6): δ (ppm) 159.43, 152.17, 148.89, 145.88,

145.02, 130.87, 130.77, 123.74, 120.40, 119.36, 119.08, 118.41, 117.78, 116.74, 34.62, 31.45; HRMS (ESI) calcd for $C_{18}H_{18}ClN_3O_2S$ $[M + H]^+$ 376.0881, found 376.0882.

1-(3-Chloro-4-hydroxyphenyl)-3-(6-ethoxybenzo[d]thiazol-2-yl)urea (63) Yield 90%; mp: 255–257 °C; 1H -NMR (300 MHz, DMSO- d_6): δ (ppm) 10.72 (br s, 1H), 9.92 (s, 1H), 9.00 (s, 1H), 7.60 (s, 1H), 7.57–7.36 (m, 2H), 7.18 (d, $J = 7.9$ Hz, 1H), 7.04–6.84 (m, 2H), 4.04 (q, $J = 6.9$ Hz, 2H), 1.33 (t, $J = 7.0$ Hz, 3H); ^{13}C -NMR (75 MHz, DMSO- d_6): δ (ppm) 157.76, 154.90, 152.19, 148.90, 141.98, 132.33, 130.82, 120.74, 119.89, 119.41, 119.34, 116.67, 114.76, 105.59, 63.59, 14.75; HRMS (ESI) calcd for $C_{16}H_{14}ClN_3O_3S$ $[M + H]^+$ 364.0517, found 364.0521.

1-(3-Chloro-4-hydroxyphenyl)-3-(6-((trifluoromethyl)thio)benzo[d]thiazol-2-yl)urea (64) Yield 24%; mp: 256–258 °C; 1H -NMR (500 MHz, DMSO- d_6): δ (ppm) 11.04 (br s, 1H), 9.95 (br s, 1H), 9.03 (s, 1H), 8.37 (d, $J = 1.8$ Hz, 1H), 7.75 (d, $J = 8.4$ Hz, 1H), 7.67 (dd, $J = 8.4, 1.9$ Hz, 1H), 7.59 (d, $J = 2.6$ Hz, 1H), 7.19 (dd, $J = 8.8, 2.6$ Hz, 1H), 6.95 (d, $J = 8.7$ Hz, 1H); ^{13}C -NMR (126 MHz, DMSO- d_6): δ (ppm) 162.27, 152.10, 150.64, 149.08, 134.08, 132.73, 130.61, 130.28, 129.69 (q, $J = 308.1$ Hz), 120.65, 120.34, 119.38, 119.33, 116.74, 115.69 (q, $J = 2.1$ Hz); HRMS (ESI) calcd for $C_{15}H_9ClF_3N_3O_2S_2$ $[M + H]^+$ 419.9850, found 419.9873.

1-(3-Chloro-4-hydroxyphenyl)-3-(6-thiocyanatobenzo[d]thiazol-2-yl)urea (65) Yield 80%; mp: 251–253 °C; 1H -NMR (500 MHz, DMSO- d_6): δ (ppm) 11.04 (br s, 1H), 9.97 (br s, 1H), 9.13 (br s, 1H), 8.32 (d, $J = 2.0$ Hz, 1H), 7.74 (d, $J = 8.5$ Hz, 1H), 7.64 (dd, $J = 8.5, 2.0$ Hz, 1H), 7.60 (d, $J = 2.6$ Hz, 1H), 7.19 (dd, $J = 8.8, 2.6$ Hz, 1H), 6.94 (d, $J = 8.7$ Hz, 1H); ^{13}C -NMR (126 MHz, DMSO- d_6): δ (ppm) 161.91, 152.15, 149.47, 149.14, 133.11, 130.46, 129.54, 125.55, 121.00, 120.73, 119.66, 119.35, 116.75, 116.66, 112.20; HRMS (ESI) calcd for $C_{15}H_9ClN_4O_2S_2$ $[M + H]^+$ 376.9928, found 376.9939.

1-(3-Chloro-4-hydroxyphenyl)-3-(6-(methylsulfonyl)benzo[d]thiazol-2-yl)urea (66) Yield 78%; mp: 293–295 °C; 1H -NMR (500 MHz, DMSO- d_6): δ (ppm) 11.16 (br s, 1H), 9.94 (br s, 1H), 9.25 (s, 1H), 8.55 (d, $J = 1.7$ Hz, 1H), 7.89 (dd, $J = 8.5, 1.9$ Hz, 1H), 7.82 (d, $J = 8.5$ Hz, 1H), 7.61 (d, $J = 2.6$ Hz, 1H), 7.20 (dd, $J = 8.8, 2.6$ Hz, 1H), 6.95 (d, $J = 8.7$ Hz, 1H), 3.23 (s, 3H); ^{13}C -NMR (126 MHz, DMSO- d_6): δ (ppm) 163.39, 152.08, 149.15, 134.69, 131.79, 130.45, 124.81, 121.71, 120.89, 119.56, 119.36, 116.68, 44.09; HRMS (ESI) calcd for $C_{15}H_{12}ClN_3O_4S_2$ $[M + H]^+$ 398.0031, found 398.0048.

1-(3-Chloro-4-hydroxyphenyl)-3-(6-((trifluoromethyl)sulfonyl)benzo[d]thiazol-2-yl)urea (67) Yield 94%; mp: 267–269 °C; 1H -NMR (300 MHz, DMSO- d_6): δ (ppm) 11.40 (br s, 1H), 10.01 (s, 1H), 9.10 (br s, 1H), 8.89 (s, 1H), 8.02 (dd, $J = 8.6, 1.9$ Hz, 1H), 7.95 (d, $J = 8.4$ Hz, 1H), 7.60 (d, $J = 2.5$ Hz, 1H), 7.21 (dd, $J = 8.7, 2.3$ Hz, 1H), 6.95 (d, $J = 8.8$ Hz, 1H); ^{13}C -NMR (75 MHz, DMSO- d_6): δ (ppm) 166.05, 155.92, 149.35, 133.47, 130.23, 128.07, 126.29, 121.75, 121.17, 119.85, 119.36, 117.44, 116.67, 40.35, 40.08, 39.80, 39.52, 39.24, 38.96, 38.69; HRMS (ESI) calcd for $C_{15}H_9ClF_3N_3O_4S_2$ $[M + H]^+$ 451.9748, found 451.9749.

1-(3-Chloro-4-hydroxyphenyl)-3-(4,5,6,7-tetrahydrobenzo[d]thiazol-2-yl)urea (71) Yield 58%; mp: 258–260 °C; 1H -NMR (500 MHz, DMSO- d_6): δ (ppm) 9.91 (br s, 1H), 7.55 (d, $J = 2.4$ Hz, 1H), 7.14 (dd, $J = 8.7, 2.4$ Hz, 1H), 6.94 (d, $J = 8.7$ Hz, 1H), 2.59 (s, 2H), 2.54 (s, 2H), 1.75 (s, 4H); ^{13}C -NMR (126 MHz, DMSO- d_6): δ (ppm) 158.38, 151.01, 149.02, 138.46, 130.54, 120.47, 120.31, 119.38, 119.00, 116.77, 24.13, 22.46, 22.07, 21.82; HRMS (ESI) calcd for $C_{14}H_{14}ClN_3O_2S$ $[M + H]^+$ 324.05680, found 324.05634.

1-(3-Chloro-4-hydroxyphenyl)-3-(2,3-dihydro-1H-inden-2-yl)urea (72) Yield 21%; mp: 203–205 °C; 1H -NMR (500 MHz, DMSO- d_6): δ (ppm) 9.59 (br s, 1H), 8.14 (br s, 1H), 7.52 (d, $J = 2.6$ Hz, 1H), 7.29–7.19 (m, 2H), 7.19–7.10 (m, 2H), 6.97 (dd, $J = 8.7, 2.6$ Hz, 1H), 6.83 (d, $J = 8.7$ Hz, 1H), 6.36 (d, $J = 7.3$ Hz, 1H), 4.48–4.31 (m, 1H), 3.25–3.09 (m, 2H), 2.84–2.67 (m, 2H); ^{13}C -NMR (126 MHz, DMSO- d_6): δ (ppm) 155.00, 147.38, 141.23, 132.93, 126.40, 124.56, 119.34, 119.16, 117.90, 116.55, 50.77, 39.70; HRMS (ESI) calcd for $C_{16}H_{15}ClN_2O_2$ $[M + H]^+$ 303.08948, found 303.08908.

1-(3-Chloro-4-hydroxyphenyl)-3-(4-(4-chlorophenyl)thiazol-2-yl)urea (73) Yield 71%; mp: 206–208 °C; 1H -NMR (500 MHz, DMSO- d_6): δ (ppm) 10.69 (s, 1H), 9.91 (s, 1H), 8.76 (s, 1H), 7.92–7.87 (m, 2H), 7.60–7.57 (m, 2H), 7.50–7.45 (m, 2H), 7.14 (dd, $J = 8.7, 2.6$ Hz, 1H), 6.93 (d, $J = 8.7$ Hz, 1H);

^{13}C -NMR (126 MHz, DMSO- d_6): δ (ppm) 159.31, 151.59, 148.87, 147.41, 133.16, 132.07, 130.69, 128.67, 127.26, 120.67, 119.34, 116.66, 107.89; HRMS (ESI) calcd for $\text{C}_{16}\text{H}_{11}\text{Cl}_2\text{N}_3\text{O}_2\text{S}$ $[\text{M} + \text{H}]^+$ 380.00218, found 380.00168.

1-(3-Chloro-4-hydroxyphenyl)-3-(thiazol-2-yl)urea (74)

Yield 74%; mp: 220–222 °C; ^1H -NMR (500 MHz, DMSO- d_6): δ (ppm) 9.83 (s, 1H), 9.81 (s, 1H), 7.56 (d, $J = 2.6$ Hz, 1H), 7.47 (dd, $J = 3.9, 1.6$ Hz, 1H), 7.20 (dd, $J = 3.8, 1.5$ Hz, 1H), 7.15 (dd, $J = 8.8, 2.6$ Hz, 1H), 6.95 (d, $J = 8.7$ Hz, 1H); ^{13}C -NMR (126 MHz, DMSO- d_6): δ (ppm) 160.49, 151.25, 149.00, 133.59, 130.64, 120.41, 119.39, 119.08, 116.78, 113.06; HRMS (ESI) calcd for $\text{C}_{10}\text{H}_8\text{ClN}_3\text{O}_2\text{S}$ $[\text{M} + \text{H}]^+$ 270.0099, found 270.0099.

1-(3-Chloro-4-hydroxyphenyl)-3-(4-methoxyphenethyl)urea (75) Yield 21%; mp: 161.5–163.5 °C; ^1H -NMR (500 MHz, DMSO- d_6): δ (ppm) 9.58 (br s, 1H), 8.29 (br s, 1H), 7.52 (d, $J = 2.5$ Hz, 1H), 7.14 (d, $J = 8.5$ Hz, 2H), 6.97 (dd, $J = 8.7, 2.5$ Hz, 1H), 6.89–6.84 (m, 2H), 6.82 (d, $J = 8.7$ Hz, 1H), 5.98 (t, $J = 5.5$ Hz, 1H), 3.72 (s, 3H), 3.33–3.19 (m, 2H), 2.66 (t, $J = 7.2$ Hz, 2H); ^{13}C -NMR (126 MHz, DMSO- d_6): δ (ppm) 157.65, 155.20, 147.32, 133.06, 131.35, 129.58, 119.37, 119.14, 117.90, 116.54, 113.78, 54.97, 40.87, 34.96; HRMS (ESI) calcd for $\text{C}_{16}\text{H}_{17}\text{ClN}_2\text{O}_3$ $[\text{M} + \text{H}]^+$ 321.10005, found 321.09967.

1-(Benzo[d]thiazol-6-yl)-3-(3-chloro-4-hydroxyphenyl)urea (76) Yield 24%; mp: 224–226 °C; ^1H -NMR (500 MHz, DMSO- d_6): δ (ppm) 9.77 (s, 1H), 9.20 (s, 1H), 8.89 (s, 1H), 8.60 (s, 1H), 8.35 (d, $J = 2.1$ Hz, 1H), 7.97 (d, $J = 8.8$ Hz, 1H), 7.60 (d, $J = 2.6$ Hz, 1H), 7.47 (dd, $J = 8.8, 2.2$ Hz, 1H), 7.11 (dd, $J = 8.7, 2.6$ Hz, 1H), 6.90 (d, $J = 8.7$ Hz, 1H); ^{13}C -NMR (126 MHz, DMSO- d_6): δ (ppm) 153.69, 152.69, 148.26, 148.17, 137.64, 134.46, 131.92, 122.92, 120.22, 119.26, 118.82, 118.11, 116.63, 110.26; HRMS (ESI) calcd for $\text{C}_{14}\text{H}_{10}\text{ClN}_3\text{O}_2\text{S}$ $[\text{M} + \text{H}]^+$ 320.0255, found 320.0264.

1,3-Bis(3-chloro-4-hydroxyphenyl)urea (78) Yield 94%; mp: 254.5–256.5 °C; ^1H -NMR (500 MHz, DMSO- d_6): δ (ppm) 9.71 (br s, 2H), 8.43 (br s, 2H), 7.54 (d, $J = 2.6$ Hz, 2H), 7.06 (dd, $J = 8.8, 2.6$ Hz, 2H), 6.87 (d, $J = 8.7$ Hz, 2H); ^{13}C -NMR (126 MHz, DMSO- d_6): δ (ppm) 152.77, 147.99, 132.14, 120.11, 119.22, 118.71, 116.59; HRMS (ESI) calcd for $\text{C}_{13}\text{H}_{10}\text{Cl}_2\text{N}_2\text{O}_3$ $[\text{M} + \text{H}]^+$ 313.01412, found 313.01361.

3.3. β -HSD10 Enzymatic Activity Assay

Purification of 17 β -HSD10 protein was performed as described in our previous work [22].

Compound screening, dose response and mechanism of inhibition experiments were performed as described in Hroch et al. 2016, with the exceptions being an alteration in assay buffer (10 mM Tris HCl (pH 7.4), 150 mM NaCl, 1 mM DTT, 0.005% Tween20, 0.01% BSA) and a change in temperature to 25 °C, to improve enzyme stability and assay reliability as compound solubility improved, as outlined in our previous work [19].

Orthogonal screening (small molecule aggregation and redox cycling experiments) was carried out as described in our previous work [19].

3.4. Lactate Dehydrogenase (LDH) Cytotoxicity Assay

Cell cytotoxicity was assessed via the measurement of lactate dehydrogenase leakage into the culture medium using a commercially available kit from Pierce (Thermo Scientific, UK, cat no. 88953). This was carried out in accordance with the kit guidelines, with the activity of LDH being calculated from the change in absorbance at 340 nm as NADH is reduced. HEK293 cells overexpressing mts17 β -HSD10 were cultured in phenol-red free media (10% FBS, 1 mM Sodium Pyruvate, 100 units Penicillin, 0.1 mg/mL Streptomycin and 2 mM L-Glutamine) and seeded at a density of 10,000 cells per well (100 μL , 96-well plates). Cells were then treated with compound of interest at 2 concentrations (25 μM and 100 μM in DMSO) in triplicate. Treated cells were then incubated at 37 °C and CO_2 (5%) for 24 hours before the LDH assay was performed as per the manufacturer's instructions. Spontaneous control (water) and maximum control (lysis buffer) used in accordance with the kit guide. Absorbance was measured at 490 nm and 680 nm using the SpectraMaxM2e spectrophotometer (Molecular Devices,

San Jose, CA, USA). The measured LDH activity was used to calculate % cytotoxicity using the following equation:

$$\% \text{ cytotoxicity} = \frac{(\text{compound treated LDH Activity} - \text{Spontaneous LDH Activity})}{(\text{Maximum LDH Activity} - \text{Spontaneous LDH Activity})} \times 100 \quad (1)$$

3.5. (–)-CHANA Assay – In Vitro Dose Response and EC₅₀ Determination

HEK293 mts17β-HSD10 cells were seeded at a density of 10,000 cells per well (100 μL, 96-well black plates, Greiner Cat no. 655090) in phenol-red free media (10% FBS, 1 mM Sodium Pyruvate, 100 units Penicillin, 0.1 mg/mL Streptomycin and 2 mM L-Glutamine). The media was removed from the cells and replaced with fresh media containing varying concentrations of compound (100 μM–0.098 μM). The fluorogenic probe (–)-CHANA was then added to each well to give a final assay concentration of 20 μM. Fluorescence was immediately measured using the FLUOstar Optima microplate reader (excitation = 380 nm, emission = 520 nm, orbital averaging = 3 mm) and the initial reaction monitored for 3–4 hours. EC₅₀ was calculated from the control - subtracted triplicates using non-linear regression (four parameters) of GraphPad Prism 5 software. Final EC₅₀ and SEM value was obtained as a mean of at least 3 independent measurements.

4. Conclusions

In summary, four novel series of benzothiazolylureas were designed and synthesised. All compounds were evaluated for 17β-HSD10 inhibitory ability in vitro, where compounds **5**, **6**, and **63** showed the most promising 17β-HSD10 inhibitory activity in our enzymatic assays, although the orthogonal screens appear to indicate that **63** could be inhibiting 17β-HSD10 in an unfavourable manner. Key structure–activity relationships have been established and further validated with a urea linker and a 4-phenolic moiety with a 3-halogen substitution confirmed to be essential for compound 17β-HSD10 inhibitory ability. Furthermore, a bulky substitution (e.g., *t*-butyl) in position 6 of the benzothiazole moiety appears to be the most promising, potentially occupying the chemical space more effectively within the binding site.

Positively the most promising compounds were also shown to have an inhibitory effect at a cellular level with limited cytotoxicity and all hit compounds display a more favourable kinetic mechanism of action (reversible mixed inhibition) to other previously published work.

These findings provide significant structural activity insight into our 17β-HSD10 inhibitor compound design and are our most promising observations to date. With further hit optimisation and neuronal cellular evaluation to determine if these compounds are protective against Aβ-mediated cytotoxicity, this could potentially lead to novel class of therapeutics for AD.

Supplementary Materials: The following are available online, Figure S1: IC₅₀ Graphs for compounds **5**, **6**, **61**, **62**, **63**, **64**, **65**, **66**, **67** and **78**, Figure S2: Hanes-Woolf kinetic plots for compounds **5**, **6** and **61**. Figure S3: Hanes-Woolf kinetic plots for compounds **62**, **63** and **64**. Figure S4: Hanes-Woolf kinetic plots for compounds **65**, **66**, **67** and **61**. Figure S5: Cellular IC₅₀ Graphs for compounds **5**, **6**, **61**, **62**, **63**, **64**, **65**, **66**, **67** and **78**. Table S1: Full primary screen compound in vitro evaluation. The research data supporting this publication can be accessed at <https://doi.org/10.17630/a9bb5ff9-b6cf-4175-9840-961d4c47651a> [23].

Author Contributions: Conceptualization, L.A., O.B., K.M. and F.J.G.-M.; Data curation, L.A. and O.B.; Formal analysis, L.A., B.E.M., R.E.H. and L.L.M.; Funding acquisition, L.A., T.K.S., K.M. and F.J.G.-M.; Investigation, L.A., O.B., B.E.M., R.E.H., L.H., M.S., L.L.M. and L.V.; Methodology, L.A., O.B. and L.H.; Resources, K.K., T.K.S., K.M. and F.J.G.-M.; Supervision, L.A., O.B., T.K.S., K.M. and F.J.G.-M.; Visualization, L.A.; Writing—original draft, L.A. and O.B.; Writing—review & editing, L.A., O.B., T.K.S. and K.M.

Funding: In the UK, this work was supported by the Wellcome Trust (204821/Z/16/Z), Alzheimer’s Society (specifically The Barcopel Foundation), Scottish Universities Life Science Alliance (SULSA), The Rosetrees Trust and RS MacDonald Charitable Trust. In the Czech Republic, this work was supported by Ministry of Education, Youth and Sports of Czech Republic (project ESF no. CZ.02.1.01/0.0/0.0/18_069/0010054), Ministry of Health of the Czech Republic (no. NV19-09-00578) and University of Hradec Kralove (Faculty of Science, no. VT2019-2021, SV2115-2018, and Postdoctoral job positions at UHK).

Conflicts of Interest: The authors declare no conflicts of interest.

References

1. Muirhead, K.E.A.; Borger, E.; Aitken, L.; Conway, S.; Gunn-Moore, F.J. The consequences of mitochondrial amyloid beta peptide in Alzheimer's disease. *Biochem. J.* **2010**, *426*, 255–270. [[CrossRef](#)] [[PubMed](#)]
2. Borger, E.; Aitken, L.; Muirhead, K.; Ainge, J.; Conway, S.; Gunn-Moore, F.J. Models for mitochondrial involvement in Alzheimer's Disease. *Biochem Soc. Trans.* **2011**, *39*, 868–873. [[CrossRef](#)] [[PubMed](#)]
3. Benek, O.; Aitken, L.; Hroch, L.; Kuca, K.; Gunn-Moore, F.; Musilek, K. A Direct interaction between mitochondrial proteins and amyloid- β peptide and its significance for the progression and treatment of Alzheimer's disease. *Curr. Med. Chem.* **2015**, *22*, 1056–1085. [[CrossRef](#)] [[PubMed](#)]
4. Yao, J.; Irwin, R.W.; Zhao, L.; Nilsen, J.; Hamilton, R.T.; Brinton, R.D. Mitochondrial bioenergetic deficit precedes Alzheimer's pathology in female mouse model of Alzheimer's disease. *Proc. Natl. Acad. Sci. USA* **2009**, *106*, 14670–14675. [[CrossRef](#)] [[PubMed](#)]
5. Lustbader, J.W.; Cirilli, M.; Lin, C.; Xu, H.W.; Takuma, K.; Wang, N.; Caspersen, C.; Chen, X.; Pollak, S.; Chaney, M.; et al. ABAD Directly Links A β to Mitochondrial Toxicity in Alzheimer's Disease. *Science* **2004**, *304*, 448–452. [[CrossRef](#)] [[PubMed](#)]
6. Lauretti, E.; Li, J.-G.; Di Meco, A.; Praticò, D. Glucose deficit triggers tau pathology and synaptic dysfunction in a tauopathy mouse model. *Transl. Psychiatry* **2017**, *7*, e1020. [[CrossRef](#)] [[PubMed](#)]
7. Lim, Y.-A.; Grimm, A.; Giese, M.; Mensah-Nyagan, A.G.; Villafranca, J.E.; Ittner, L.M.; Eckert, A.; Götz, J. Inhibition of the Mitochondrial Enzyme ABAD Restores the Amyloid- β -Mediated Dereglulation of Estradiol. *PLoS ONE* **2011**, *6*, e28887. [[CrossRef](#)] [[PubMed](#)]
8. Valasani, K.R.; Sun, Q.; Hu, G.; Li, J.; Du, F.; Guo, Y.; Carlson, E.A.; Gan, X.; Yan, S.S. Identification of Human ABAD Inhibitors for Rescuing A β -Mediated Mitochondrial Dysfunction. *Curr. Alzheimer Res.* **2014**, *11*, 128–136. [[CrossRef](#)]
9. Hroch, L.; Benek, O.; Guest, P.; Aitken, L.; Soukup, O.; Janockova, J.; Musil, K.; Dohnal, V.; Dolezal, R.; Kuca, K.; et al. Design, synthesis and in vitro evaluation of benzothiazole-based ureas as potential ABAD/17 β -HSD10 modulators for Alzheimer's disease treatment. *Bioorganic Med. Chem. Lett.* **2016**, *26*, 3675–3678. [[CrossRef](#)]
10. Hroch, L.; Guest, P.; Benek, O.; Soukup, O.; Janockova, J.; Dolezal, R.; Kuca, K.; Aitken, L.; Smith, T.K.; Gunn-Moore, F.; et al. Synthesis and evaluation of frentizole-based indolyl thiourea analogues as MAO/ABAD inhibitors for Alzheimer's disease treatment. *Bioorganic Med. Chem.* **2017**, *25*, 1143–1152. [[CrossRef](#)]
11. Benek, O.; Hroch, L.; Aitken, L.; Dolezal, R.; Guest, P.; Benkova, M.; Soukup, O.; Musil, K.; Hughes, R.; Kuca, K.; et al. 6-benzothiazolyl ureas, thioureas and guanidines are potent inhibitors of ABAD/17 β -HSD10 and potential drugs for Alzheimer's disease treatment: Design, synthesis and in vitro evaluation. *Med. Chem.* **2017**, *13*, 345–358. [[CrossRef](#)]
12. Xiao, X.; Chen, Q.; Zhu, X.; Wang, Y. ABAD/17 β -HSD10 reduction contributes to the protective mechanism of huperzine A on the cerebral mitochondrial function in APP/PS1 mice. *Neurobiol. Aging* **2019**, *81*, 77–87. [[CrossRef](#)] [[PubMed](#)]
13. Du Yan, S.; Fu, J.; Soto, C.; Chen, X.; Zhu, H.; Al-Mohanna, F.; Collison, K.; Zhu, A.; Stern, E.; Saido, T.; et al. An intracellular protein that binds amyloid- β peptide and mediates neurotoxicity in Alzheimer's disease. *Nature* **1997**, *389*, 689–695. [[CrossRef](#)] [[PubMed](#)]
14. Yao, J.; Taylor, M.; Davey, F.; Ren, Y.; Aiton, J.; Coote, P.; Fang, F.; Chen, J.X.; Yan, S.D.; Gunn-Moore, F.J. Interaction of amyloid binding alcohol dehydrogenase/Abeta mediates up-regulation of peroxiredoxin II in the brains of Alzheimer's disease patients and a transgenic Alzheimer's disease mouse model. *Mol. Cell. Neurosci.* **2007**, *35*, 377–382. [[CrossRef](#)] [[PubMed](#)]
15. Oppermann, U.C.T.; Salim, S.; Tjernberg, L.O.; Terenius, L.; Jörnvall, H. Binding of amyloid β -peptide to mitochondrial hydroxyacyl-CoA dehydrogenase (ERAB): Regulation of an SDR enzyme activity with implications for apoptosis in Alzheimer's disease. *FEBS Lett.* **1999**, *451*, 238–242. [[CrossRef](#)]
16. Du Yan, S.; Shi, Y.; Zhu, A.; Fu, J.; Zhu, H.; Zhu, Y.; Gibson, L.; Stern, E.; Collison, K.; Al-Mohanna, F.; et al. Role of ERAB/l-3-Hydroxyacyl-coenzyme A Dehydrogenase Type II Activity in A β -induced Cytotoxicity. *J. Biol. Chem.* **1999**, *274*, 2145–2156. [[CrossRef](#)] [[PubMed](#)]

17. Valasani, K.R.; Hu, G.; Chaney, F.O.; Yan, W.S.S. Structure Based Design and Synthesis of Benzothiazole Phosphonate Analogues with Inhibitors of Human ABAD-A β for Treatment of Alzheimer's Disease. *Chem. Biol. Drug Des.* **2013**, *81*, 238–249. [[CrossRef](#)] [[PubMed](#)]
18. Yan, J.G.; Tang, R.Y.; Zhong, P.; Li, J.H. Copper-catalysed tandem reactions of 2-halobenzenamines with isothiocyanates under ligand- and base-free conditions. *Tetrahedron Lett.* **2010**, *51*, 649–652.
19. Aitken, L.; Baillie, G.; Pannifer, A.; Morrison, A.; Jones, P.; Smith, T.; McElroy, S.; Gunn-Moore, F. In Vitro Assay Development and HTS of Small Molecule Human ABAD/17 β -HSD10 Inhibitors as Therapeutics in Alzheimer's Disease. *SLAS Discov.* **2017**, *22*, 676–685. [[CrossRef](#)]
20. Kissinger, C.R.; Rejto, P.A.; Pelletier, L.A.; Thomson, J.A.; Showalter, R.E.; Abreo, M.A.; Agree, C.S.; Margosiak, S.; Meng, J.J.; Aust, R.M.; et al. Crystal Structure of Human ABAD/HSD10 with a Bound Inhibitor: Implications for Design of Alzheimer's Disease Therapeutics. *J. Mol. Biol.* **2004**, *342*, 943–952. [[CrossRef](#)]
21. Muirhead, K.E.A.; Froemming, M.; Li, X.; Musilek, K.; Conway, S.J.; Sames, D.; Gunn-Moore, F.J. (–)-CHANA, a Fluorogenic Probe for Detecting Amyloid Binding Alcohol Dehydrogenase HSD10 Activity in Living Cells. *ACS Chem. Biol.* **2010**, *5*, 1105–1114. [[CrossRef](#)] [[PubMed](#)]
22. Aitken, L.; Quinn, S.D.; Perez Gonzalez, D.C.; Samuel, I.D.W.; Penedo-Esteiro, J.C.; Gunn-Moore, F.J. Morphology-specific inhibition of β -amyloid aggregates by 17 β -hydroxysteroid dehydrogenase type 10. *ChemBioChem* **2016**, *17*, 1029–1037. [[CrossRef](#)] [[PubMed](#)]
23. Aitken, L.; Benek, O.; McKelvie, B.; Hughes, R.; Hroch, L.; Major, L.L.; Kuca, K.; Smith, T.K.; Musilek, K.; Gunn-Moore, F.J. *Data Underpinning: Novel Benzothiazole-Based Ureas as 17 β -HSD10 Inhibitors, a Potential Alzheimer's Disease Treatment. Dataset*; University of St. Andrews, Research Portal: St. Andrews, Scotland, 2018. [[CrossRef](#)]

Sample Availability: Samples of all the final compounds are available from the authors.



© 2019 by the authors. Licensee MDPI, Basel, Switzerland. This article is an open access article distributed under the terms and conditions of the Creative Commons Attribution (CC BY) license (<http://creativecommons.org/licenses/by/4.0/>).